Particle Detectors

Their principles and applications

June 26-27 2018
at Pohang Korea
Takao Inagaki (KEK)

Contents of this lecture

- 1. Introduction
  - Self introduction
  - Particle interaction with matter
- 2. Track measurement
  - Gas chamber
  - Semiconductor
- 3. dE/dx measurement
  - Scintillator
  - Calorimeter
- 4. Examples and discussions
  - Magnetic spectrometer
  - ν detectors
  - Comments

References

：books from which tables or figures are cited

- 「Detectors for particle radiation」 K. Kleinknecht (Mainz)
  Cambridge Univ. Press 1986 **K K**

- 「「Radiation detection and measurement」 G. F. Knoll (Michigan)
  John Wiley and Sons 1979 **Knoll**

- 「Review of Particle Physics」 Particle Data Group
  Chinese Physics C 40 2016 **P D G**

- 「Principles of Operation of Multi Wire Proportional and Drift Chambers」
  F. Sauli, CERN 77-9 1977 **Sauli**

1. Introduction

1-1 Self introduction

I have performed three search-for experiments at KEK 12 GeV proton synchrotron.

E64 in 1980's "search for glue-ball"

E137 in 1990's "search for lepton flavor violation"

E391a in 2000's "search for direct CP violation" succeeded by KOTO at JPARC

Large solid angle for multi-tracks.
Charged and gamma spectrometer.

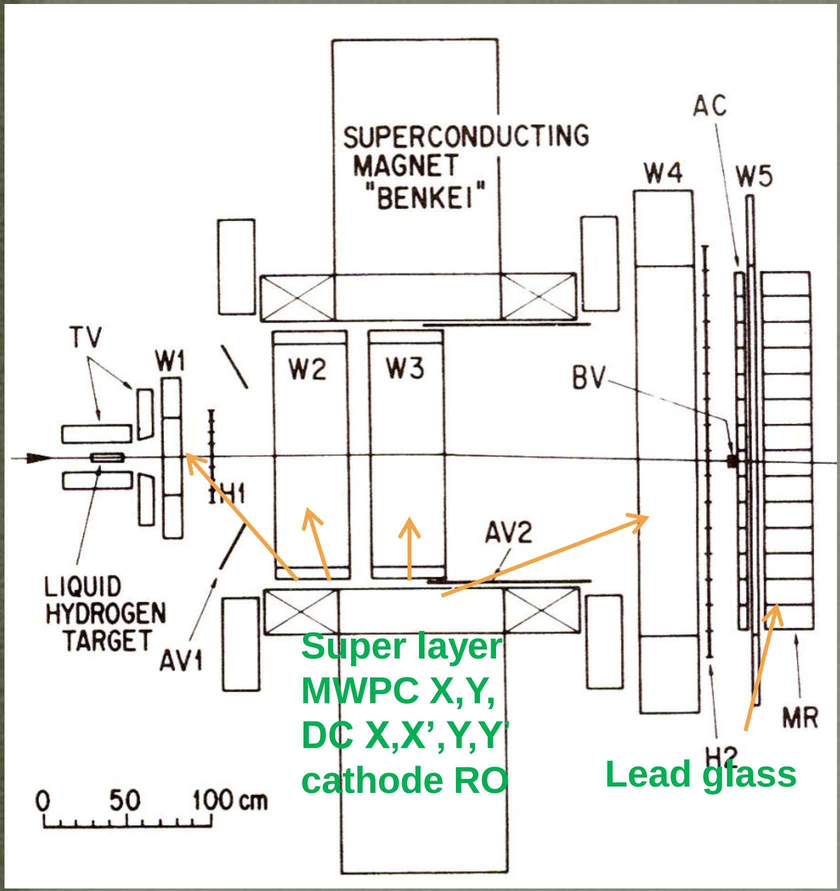

E64

Search for glueball

$\pi^- p \rightarrow M^0 n$

$M^0 \rightarrow \eta\pi^+\pi^-$

$\eta \rightarrow \gamma\gamma$

$\rightarrow \pi^0\pi^+\pi^-$

$\pi^0 \rightarrow \gamma\gamma$

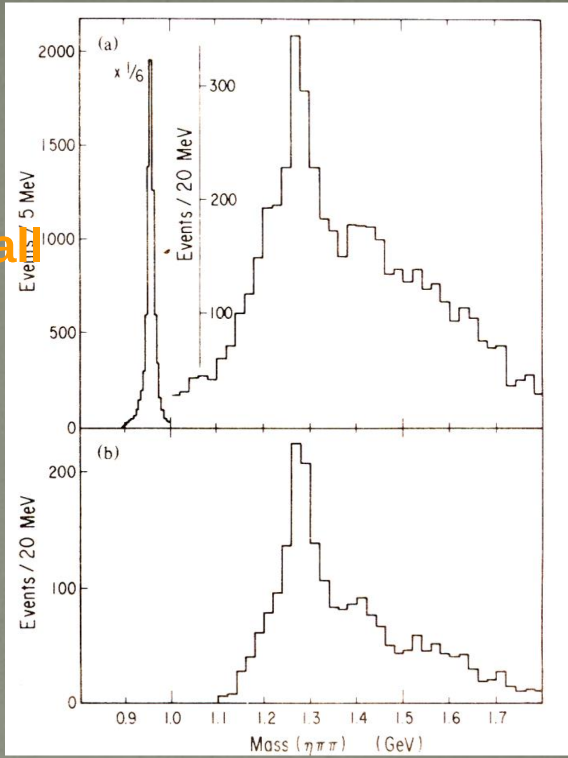

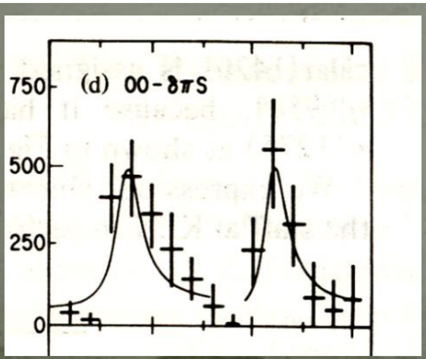

We observed two pseudo-scalar resonances which are consistent with radial excited states of η and η', and killed a possibility of the glue ball assignment to the state of 1420 MeV.

E137 $K_L \to \mu e$, $\mu\mu$, ee and eeee

High sensitivity (10^{-11}BR) ~ heavy backgrounds

Double-arm spectrometer , two stage spectrometer

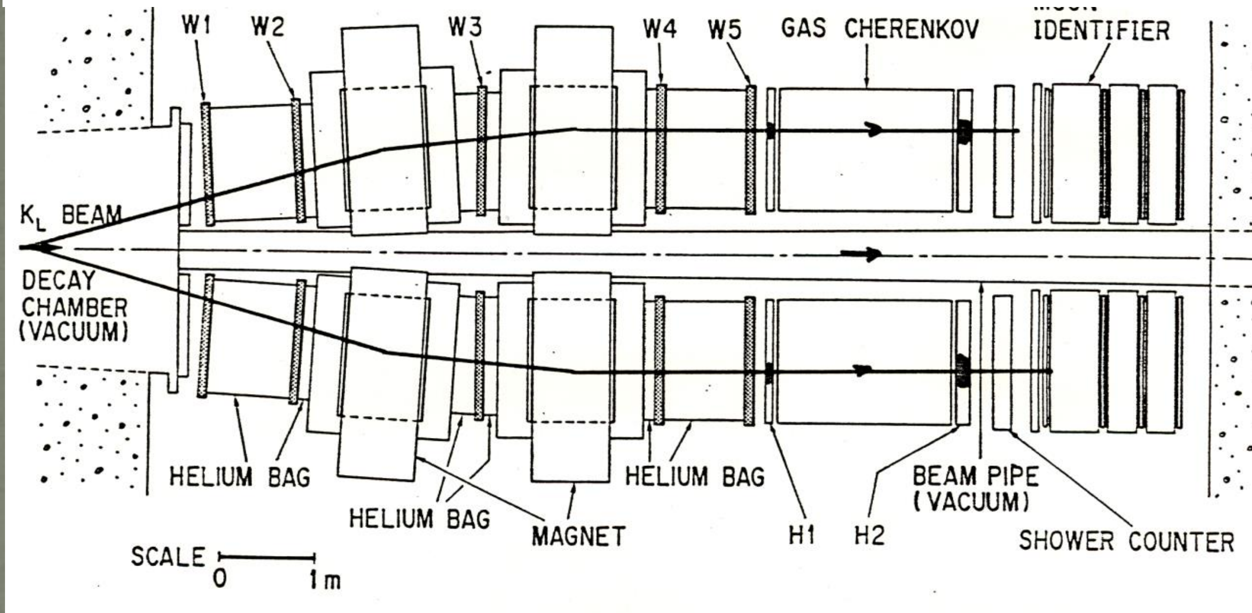

High rate: thin material to reduce n, γ interactions, He-bags, very thin vacuum window.

Wi: Drift Chamber X, X', Y, Y, no separation, Aluminum wire,

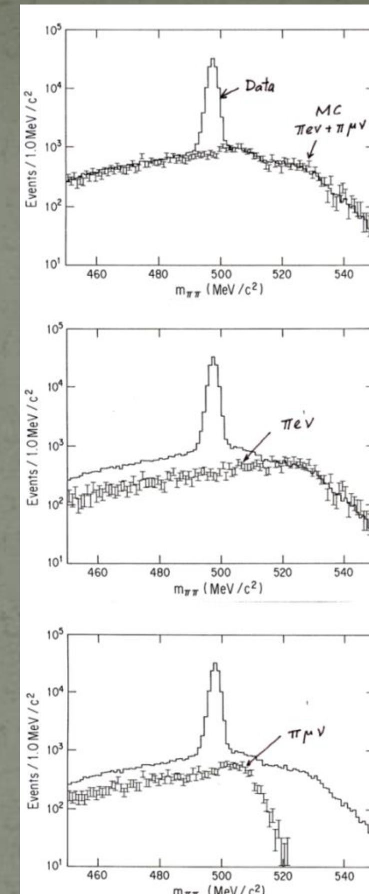

$\pi^+\pi^-$ mass

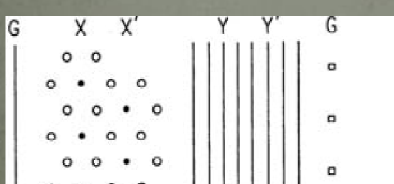

○ cathode (Al)

• sense wire (W)

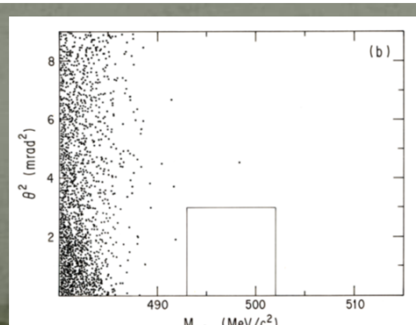

With a good mass resolution of 1.4 MeV, the upper limit 9.4 ×10^{-11} was set and it was the world record for two years .

Mostly ruled out the Technicolor Model.

E391a $K_L \rightarrow \pi^0\nu\nu$

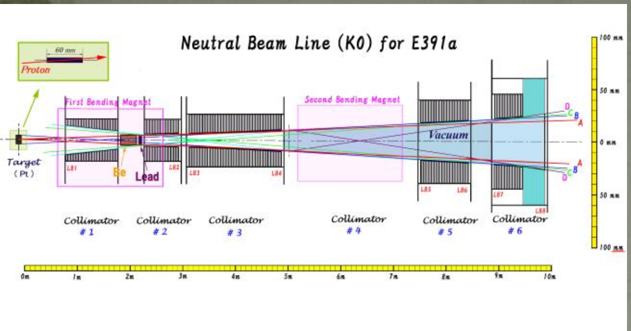

High sensitivity (heavy background) and a little kinematical constraint :
thin and sharp beam, detector in vacuum, tight veto.(full coverage and low threshold).

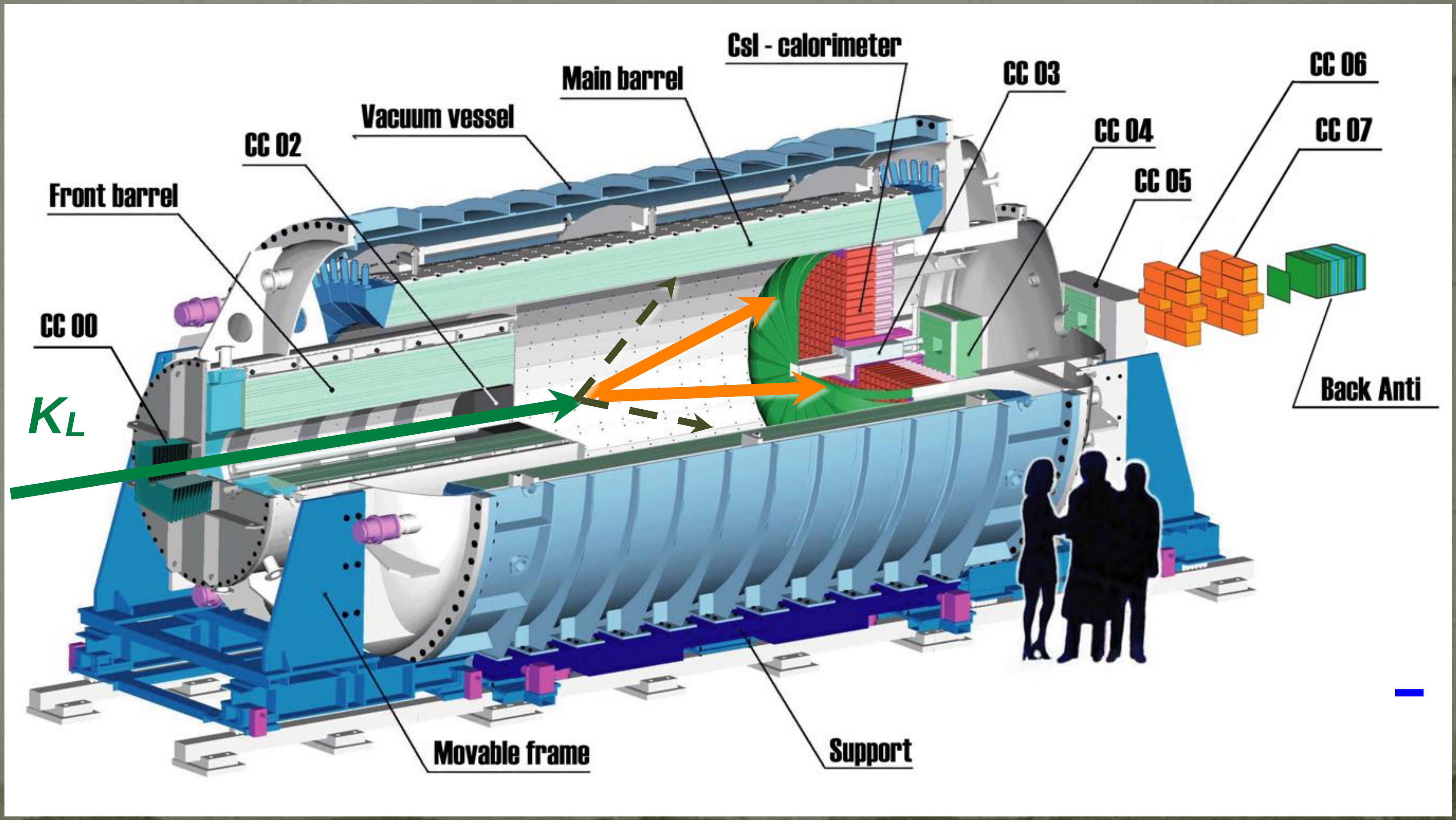

Summary of three experiments

- E64: multi-particle (track) measurements with the charge-gamma spectrometer
  - Large aperture using superconducting magnet
  - Super-layer structure of position
- E137: high resolution under high rate environment
  - Two-arm spectrometer
  - Thin materials in the upstream part
- E391a: super-sensitive vetoing
  - Sharply-collimated neutral beam
  - Detectors in vacuum

Introductory message

Even from examples of these few experiences,

"Detector is closely relate with physics, like as a telescope for astronomer. Deep world can only be explored with well polished detectors"

Classification

Medium

Measurement (Application)

Gas chamber

Scintillator

Semi-conductor

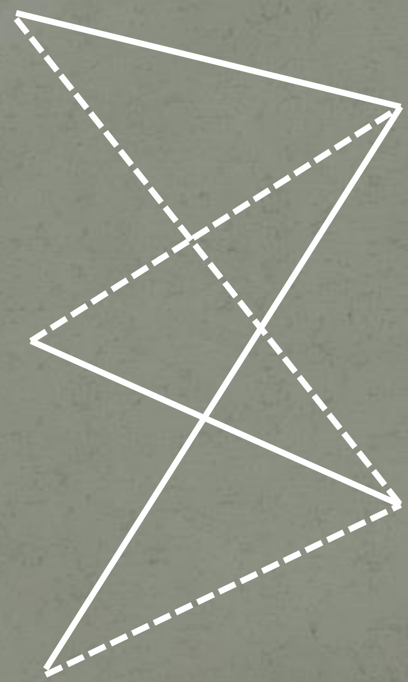

Track measurement

(Spectrometer: momentum, direction, vertex)

dE/dx measurement

(calorimeter, particle-ID)

1-2 Particle interaction with matter

- **Charged particle interaction with matter (ionization) is utilized for particle detector.**
- **Neutral particles （n ,γ ,ν） have to be converted to charged particle through production interaction with matter.**

Strong, Electromagnetic and Weak interactions

Interactions to convert **n,γ ,ν** to charged particles

n : Strong interaction

$$\mathbf{n} + \mathrm{A} \rightarrow (\pi^{\pm}, \mathbf{p}, \mathbf{n}, \pi^{0}\ (\gamma)\ \ldots) + \mathrm{A}'$$

γ : Electro-magnetic interaction

$\gamma + \mathbf{e}\ (\mathrm{A}) \rightarrow \mathbf{e} + \mathrm{A}'$; Photo-electron emission

$\gamma + \mathbf{e} \rightarrow \gamma + \mathbf{e}$; Compton scattering

$\gamma + \mathrm{A} \rightarrow \mathbf{e}^{+}\mathbf{e}^{-}\mathrm{A}$; Pair creation

[$\mathbf{e} + \mathrm{A} \rightarrow \mathbf{e} + \gamma + \mathrm{A}$;Bremstrahlung ⇒ Cascade shower]

ν : Weak interaction

$\nu_{e,\mu} + \mathrm{A} \rightarrow \mathbf{e}, \mu + \mathrm{A}'$; Charged current

$\nu_{e,\mu} + \mathrm{A} \rightarrow \nu_{e,\mu} + (\pi^{\pm}, \mathbf{p}, \mathbf{n}, \pi^{0}\ (\gamma)\ .)$; Neutral current

$\nu_{e} + \mathbf{e} \rightarrow \nu_{e} + \mathbf{e}$; Electron scattering

Strong interaction: Cross section of pp interaction

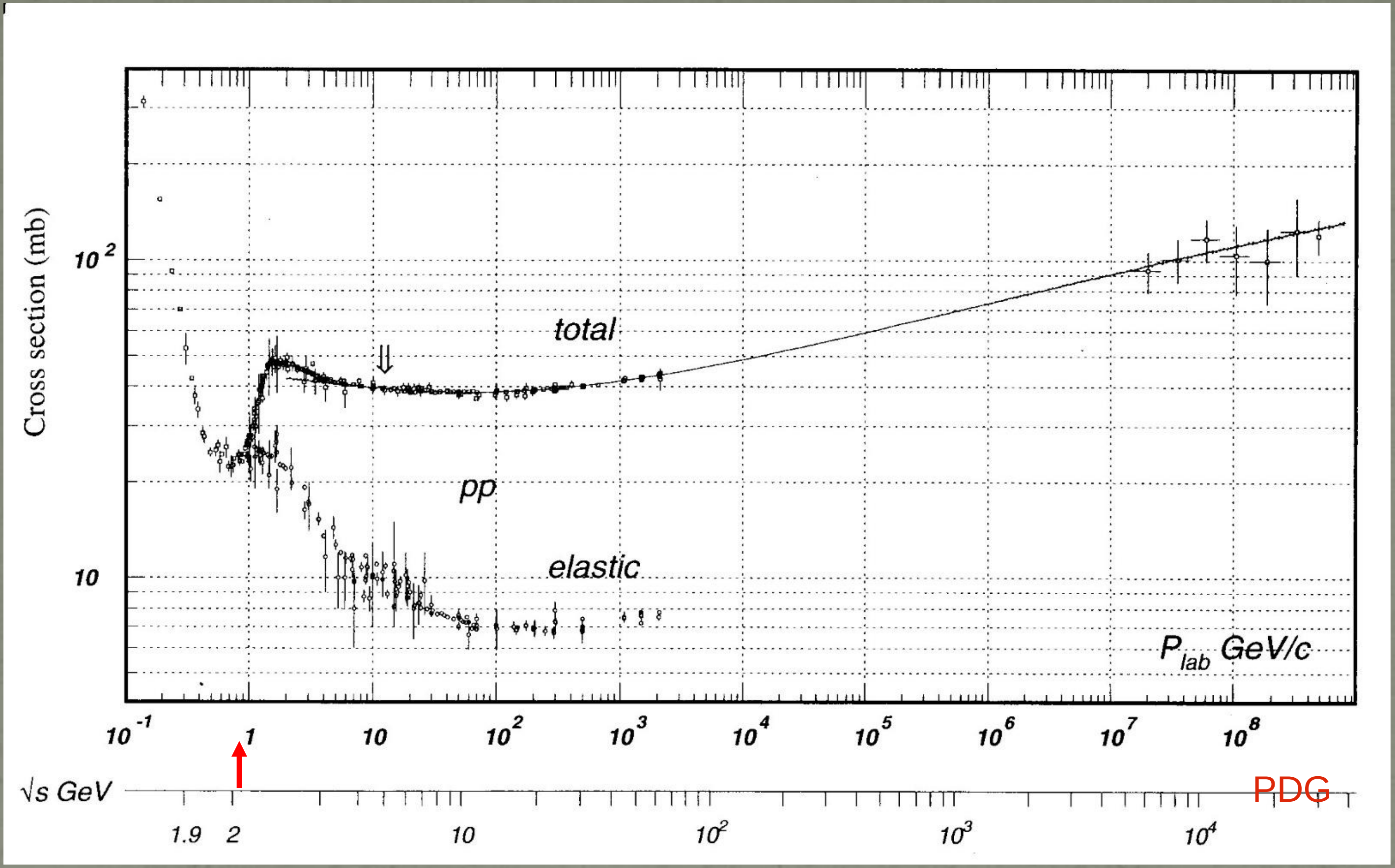

π

threshold :

$(E_p+m_p)^2 - p_{Lab}^2 = s = (2m_p + m_\pi)^2$,

$E_p^2 = p_p^2 + m_p^2$

pp ~ pn ~ nn: $\sigma_A \sim A\sigma_N$

⇒ Interaction rate ∽ thickness in the unit of gr/cm^2

Energy-independent cross section

⇒ can define **nuclear-interaction-length**

for E > 1 GeV reactions

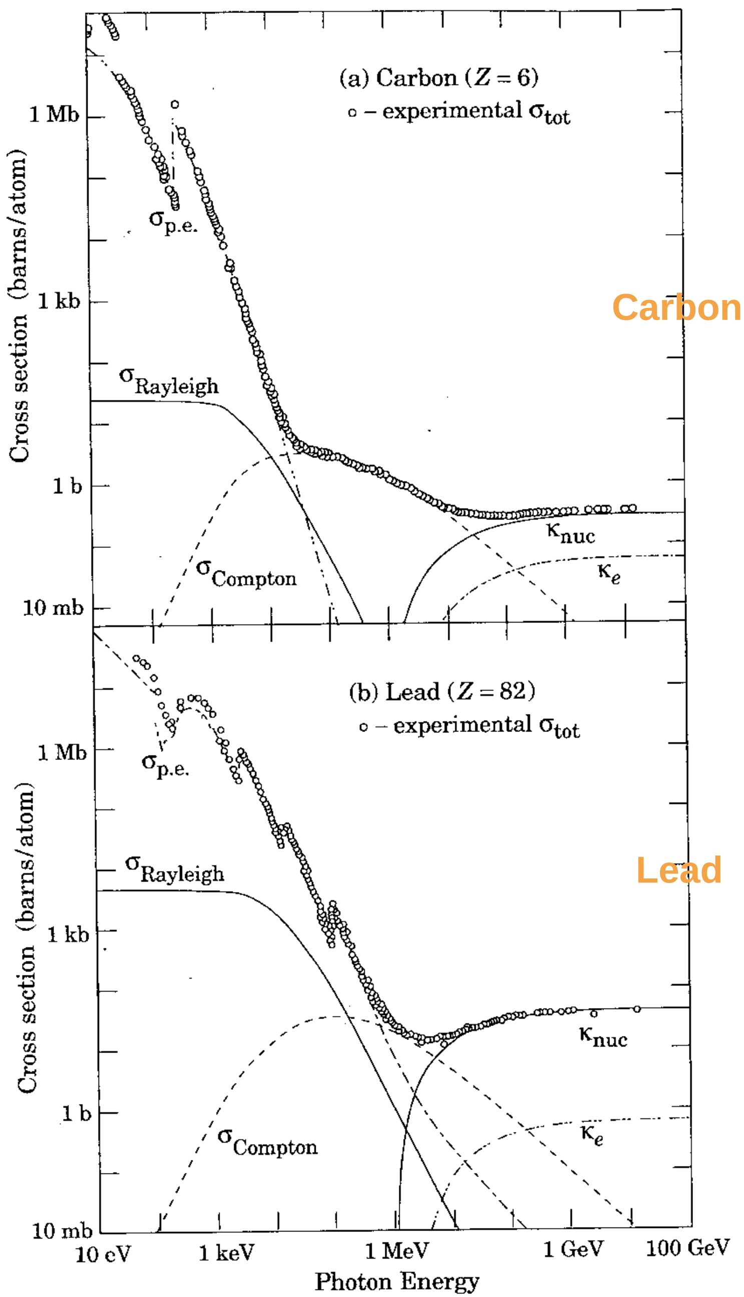

PDG

E-M interaction

Cross section of photon

Photo-electron emission (p.e.) $\propto$ Z^5

Compton scattering (Compton) $\propto$ Z

Pair creation (Knuc) $\propto$ Z^2

Effect of Compton scattering is large for light material around the energy of MeV.

Pair creation is dominant for E＞10MeV and its cross section is energy independent. ⇒ can define **radiation-length**

More exactly, the definition of radiation length comes from the facts:

1. Pair-creation (γ＋A → e^+e^-A) is dominant and the cross section is constant with energy above 10MeV.

2. Pair creation from photon (γ＋A → e^+e^-A) and bremsstrahlung of electron (positron) (e＋A → e＋γ＋A) are the same process.

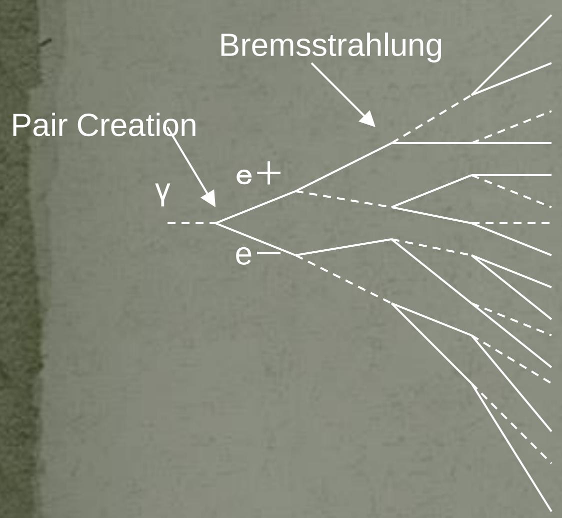

Equal mean-free-path (~radiation length [X_0]) for γ and $e^\pm$ of any energy.

Cascade shower in a medium

When the thick medium (>10 X_0) is a detector, it is calorimeter.

Incident energy (E) $\propto$ Sum of deposit energies of $e^\pm$ in the detector $\propto$ Total track length of $e^\pm$ because of the energy independent dE/dx $\propto$ The number of PC and B processes (Nproc) because of equal mean-free-path

Fluctuation $\Delta E/E \propto 1/\sqrt{Nproc} \propto 1/\sqrt{E}$

Preference of heavy material :

1.Small size due to shorter radiation length.

2.More chance of PC and B processes because heavy material is productive down to low energy.

Weak interaction: Charged-current cross section of $\nu_\mu p$

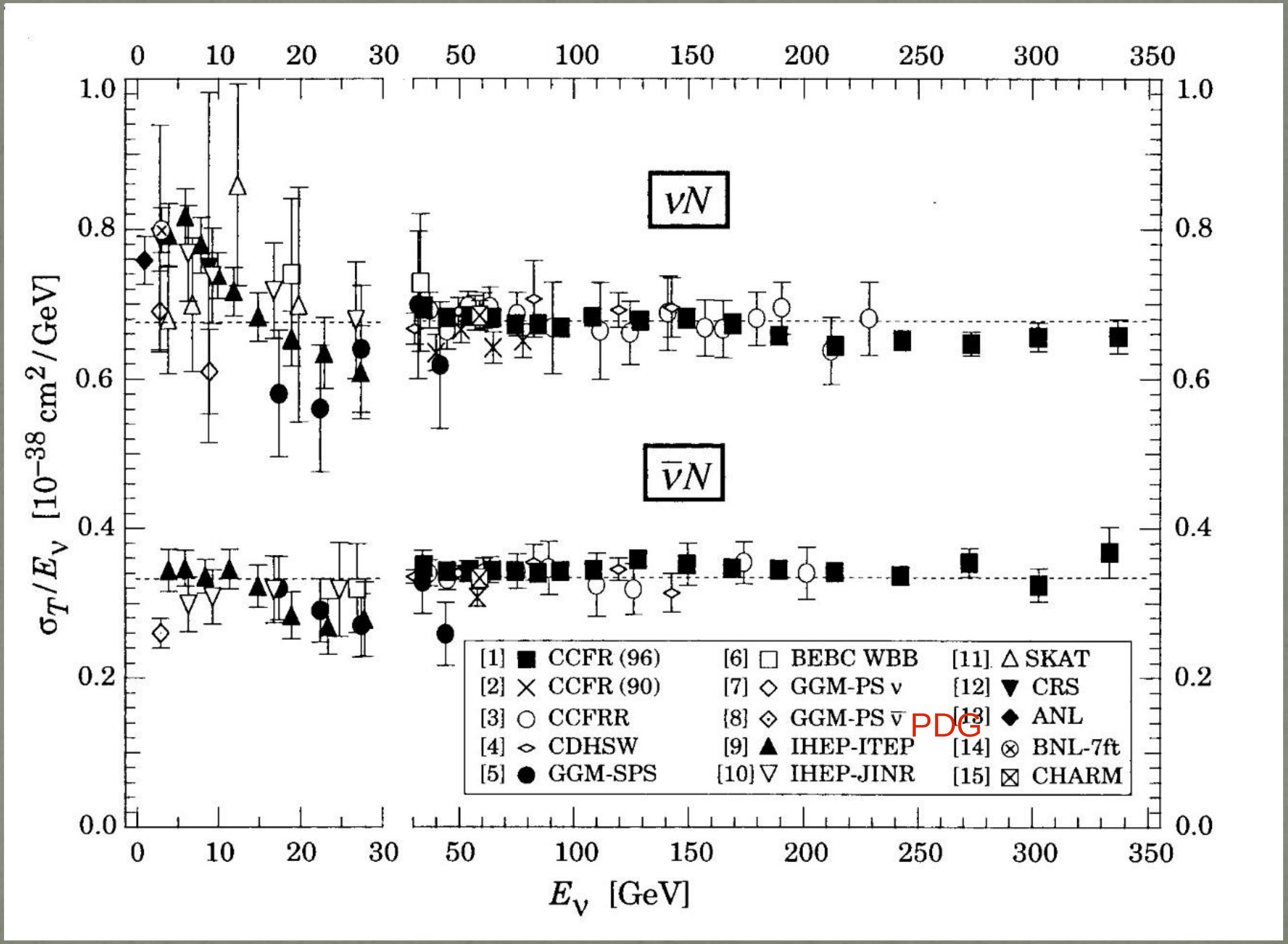

Charged-particle interaction with material

which basically determines detector response

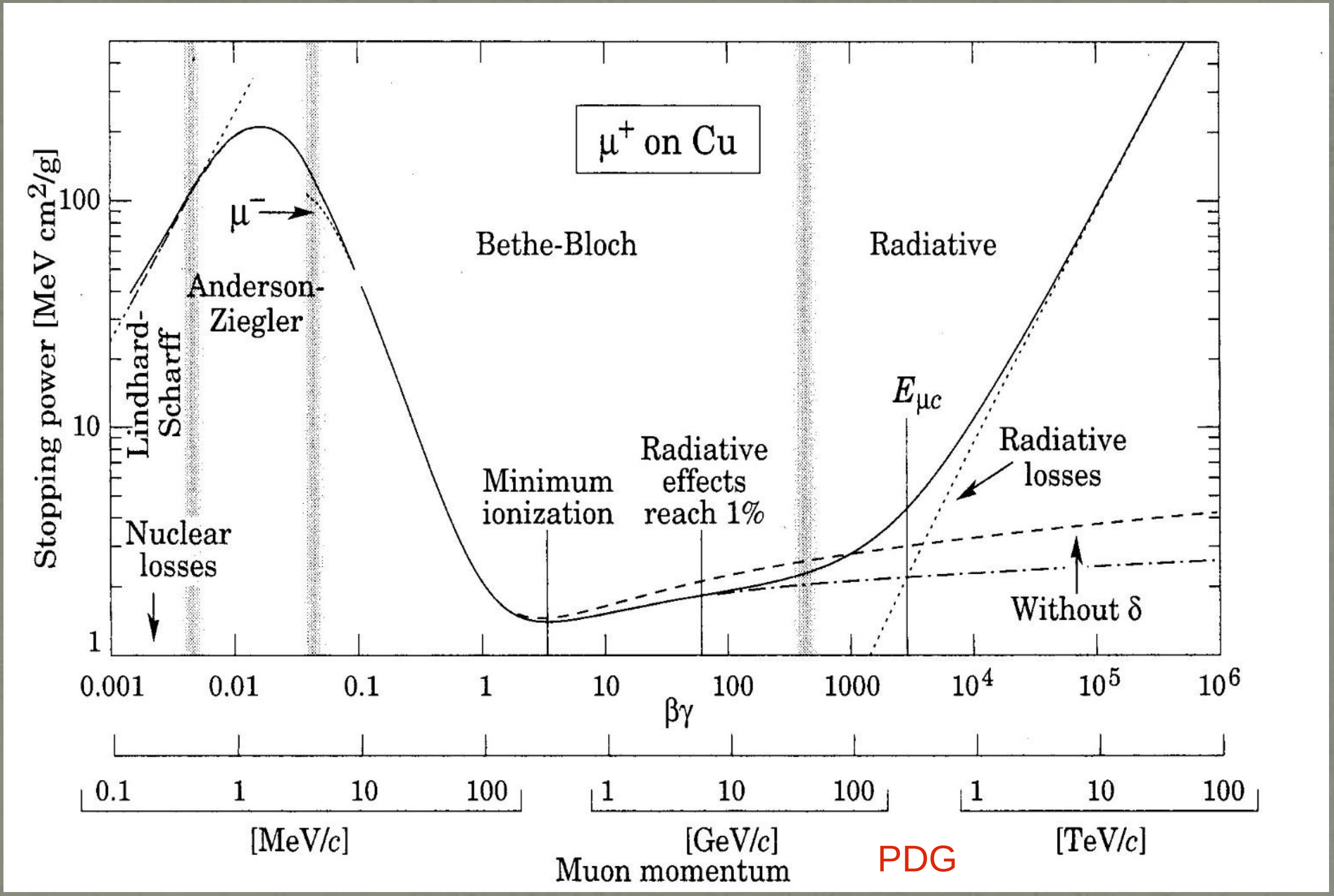

No particle dependence and single function of β and γ (velocity) in Bethe-Bloch region. The dE/dx is almost flat in the region of βγ=1~1000 with the minimum of dE/dx~2 MeV/(g/cm^2).

Bethe-Bloch formula : well-reproduce the dE/dx of the particle in the velocity region of particle nuclear physics.

$$-dE/dx = Kz^2(Z/A)(1/\beta^2)[1/2\ln\{2mc^2\gamma^2\beta^2 T_{max} / I\} - \beta^2 - \delta/2]$$

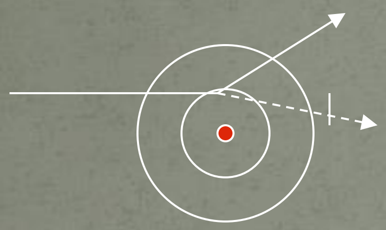

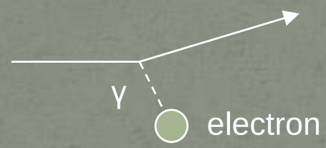

Rutherford scattering

Number of target electrons in 1gr/cm^2: $N_A \cdot Z / A$

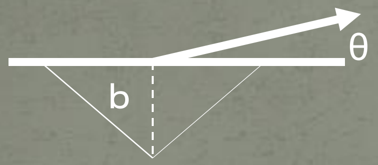

b; impact parameter

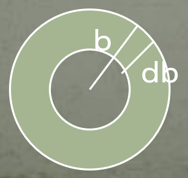

$$\Delta p = \int F dt = ze^2 / (4\pi\varepsilon_0 b^2) \cdot 2b / v$$

$$\Delta p = p \cdot \theta$$

$$b = ze^2 / (2\pi\varepsilon_0\ vp) \cdot 1/\theta$$

$$db = ze^2 / (2\pi\varepsilon_0\ vp) \cdot 1/\theta^2\, d\theta$$

$$d\sigma = 2\pi b\, db$$

$$= 2\pi\{ze^2 / (2\pi\varepsilon_0\ vp)\}^2 \cdot 1/\theta^3\, d\theta$$

$$T_e = (\Delta p)^2 / 2m = (p^2 / 2m)\, \theta^2$$

Bethe-Bloch formula (continued)

$$-dE/dx = Kz^2(Z/A)(1/\beta^2)[1/2\ln\{2mc^2\gamma^2\beta^2 T_{max} / I\} - \beta^2 - \delta/2]$$

Energy loss in 1 gr /cm^2

$-dE / dx = N_A Z / A \int_{\theta min}^{\theta max} T(\theta)(d\sigma / d\theta) d\theta$

$= K z^2 (Z / A)(1/\beta^2) \ln(\theta max / \theta min)$

$K/A = 4\pi N_A r_e^2 mc^2/A = 0.307075$ MeV/(g/cm^2)

for A=1 g/mol

$r_e = e^2/(4\pi\varepsilon_0^2 mc^2)$;   electron (classical) radius

=2.817940325(28) fm

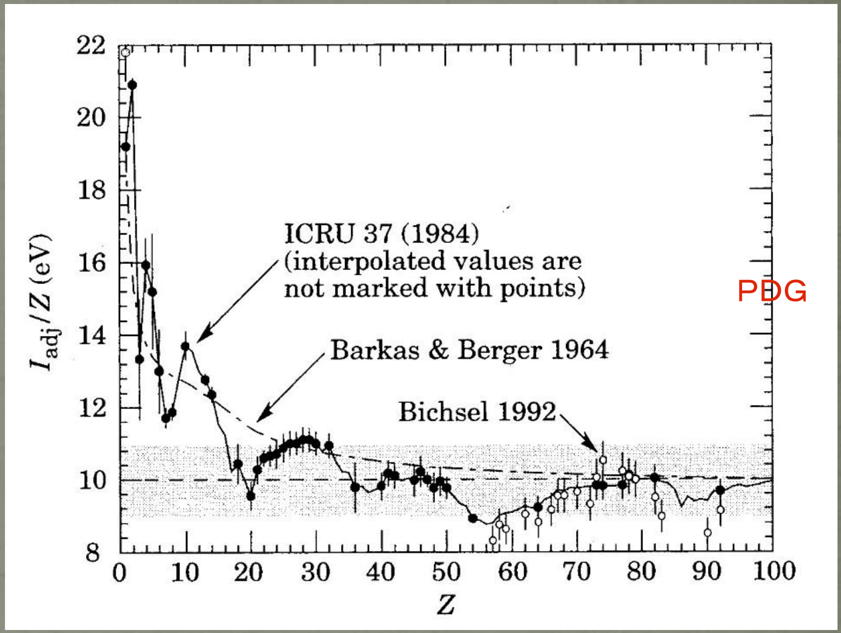

$\Theta = (2mT)^{1/2} / p$

$\ln(\theta Max / \theta Min) = (1/2) \ln(T_{max} / T_{min})$

Tmin; $I = p^2 / 2m - (p - \triangle p_{min})^2 / 2M = (p / m) \triangle p_{min}$

$T_{min} = (\triangle p_{min})^2 / 2m = (m^2 / p^2)(I / m)$

$p = \beta\gamma m c$

$\ln(\theta Max / \theta Min) = (1/2) \ln(2mc^2\beta^2\gamma^2 T_{max} / I)$

Cosmic ray flux with the altitude

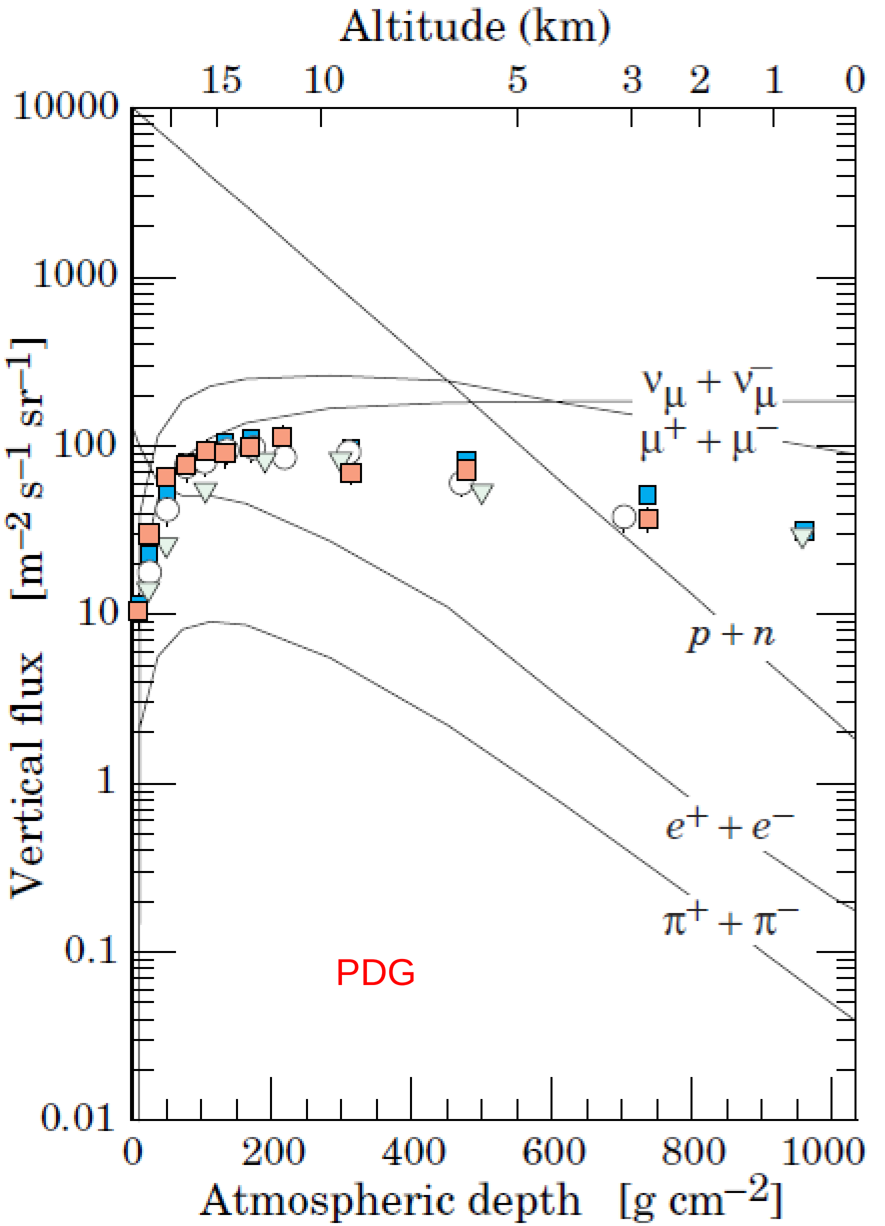

Figure 30.4: Vertical fluxes of cosmic rays in the atmosphere with $E > 1$ GeV estimated from the nucleon flux of Eq. (30.2). The points show measurements of negative muons with $E_\mu > 1$ GeV [41–45].

2. Track measurement

Gas chamber

Contents

- Seeds and multiplication
- Gas selection
- Drift velocity
- Example
- Problems: positive ion, diffusion,
- TPC

Seed

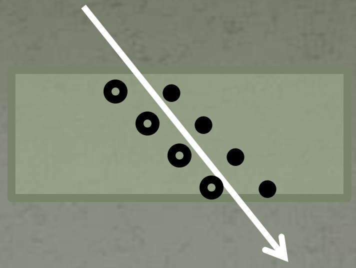

Seed: electron-ion pairs in the gas.

The Number of seed ＝deposit energy in the gas / W

- W is the required energy deposit for one pair: it is not so varied with incident particles and gas. It is around 30 eV.
- Deposit energy in Argon gas of 1 cm thick

energy loss = 2 MeV/(gr/cm^2)

material thickness : 40 g /(22.4 × 10^3)cm^3 × 1 cm

= 1.8 × 10^{-3} gr/cm^2

= 2 MeV/(gr/cm^2) × 1.8 × 10^{-3} gr/cm^2 = **3.6 keV**

Then, the number of seed ＝**120**

Capacitive readout with 100 pF 120 × 1.6 × 10^{-19}/(100 × 10^{-12}) =1.9 × 10^{-7} V

Current through 0.1 μsec propagation 120 × 1.6 × 10^{-19}/(1 × 10^{-7}) =1.9 × 10^{-10} A

Too small. Necessary for signal amplification

Multiplication in gas

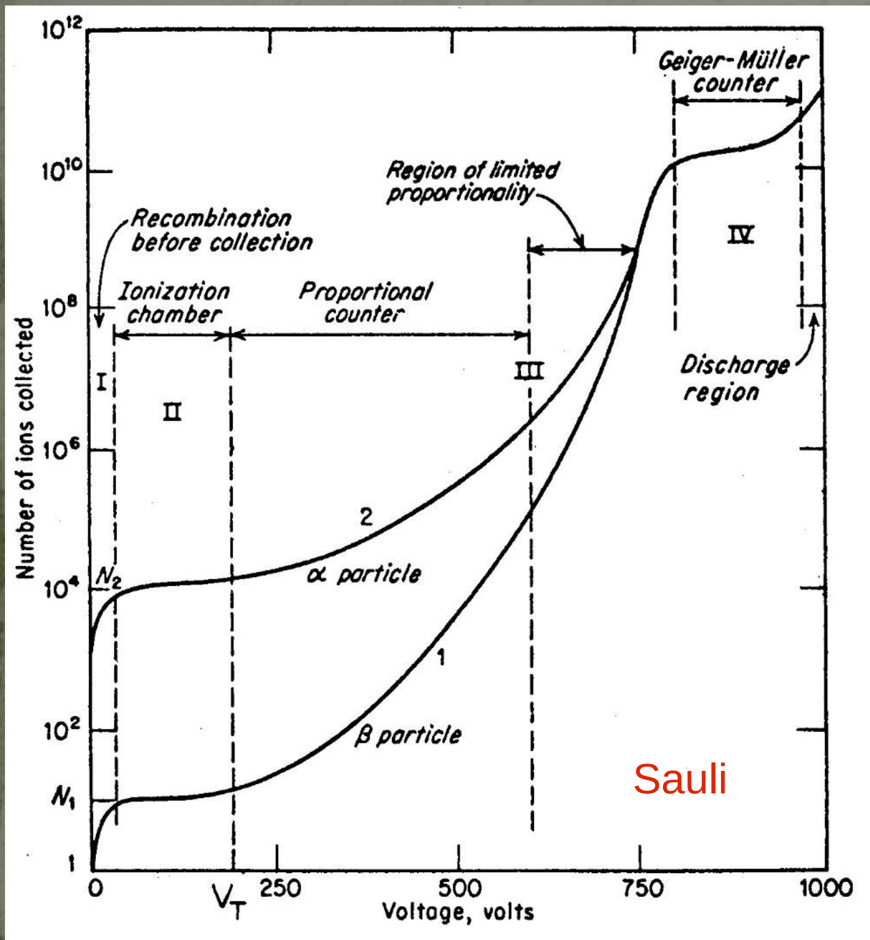

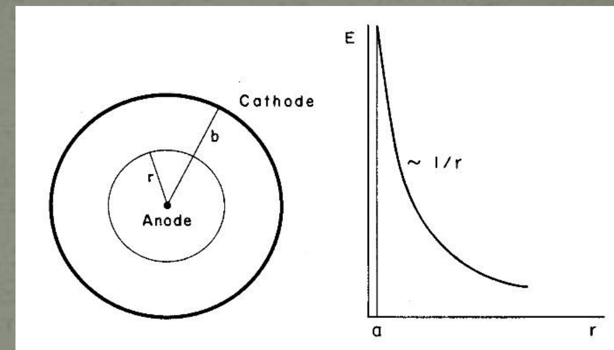

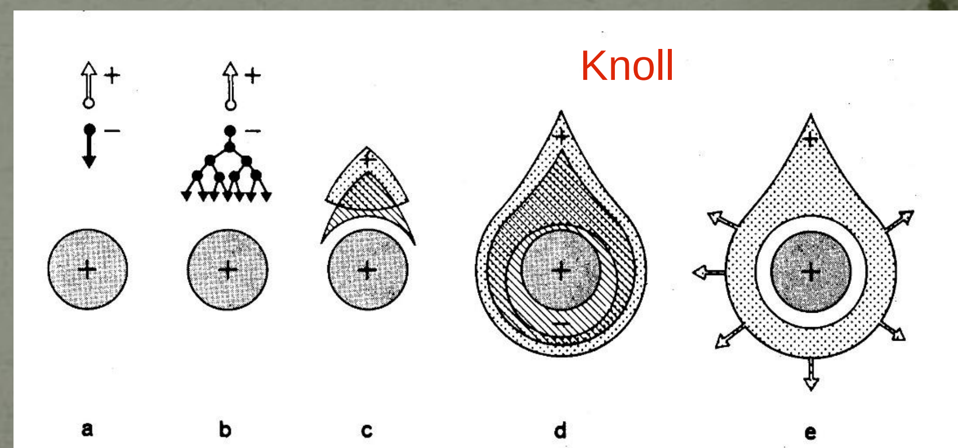

Giger-Muller counter

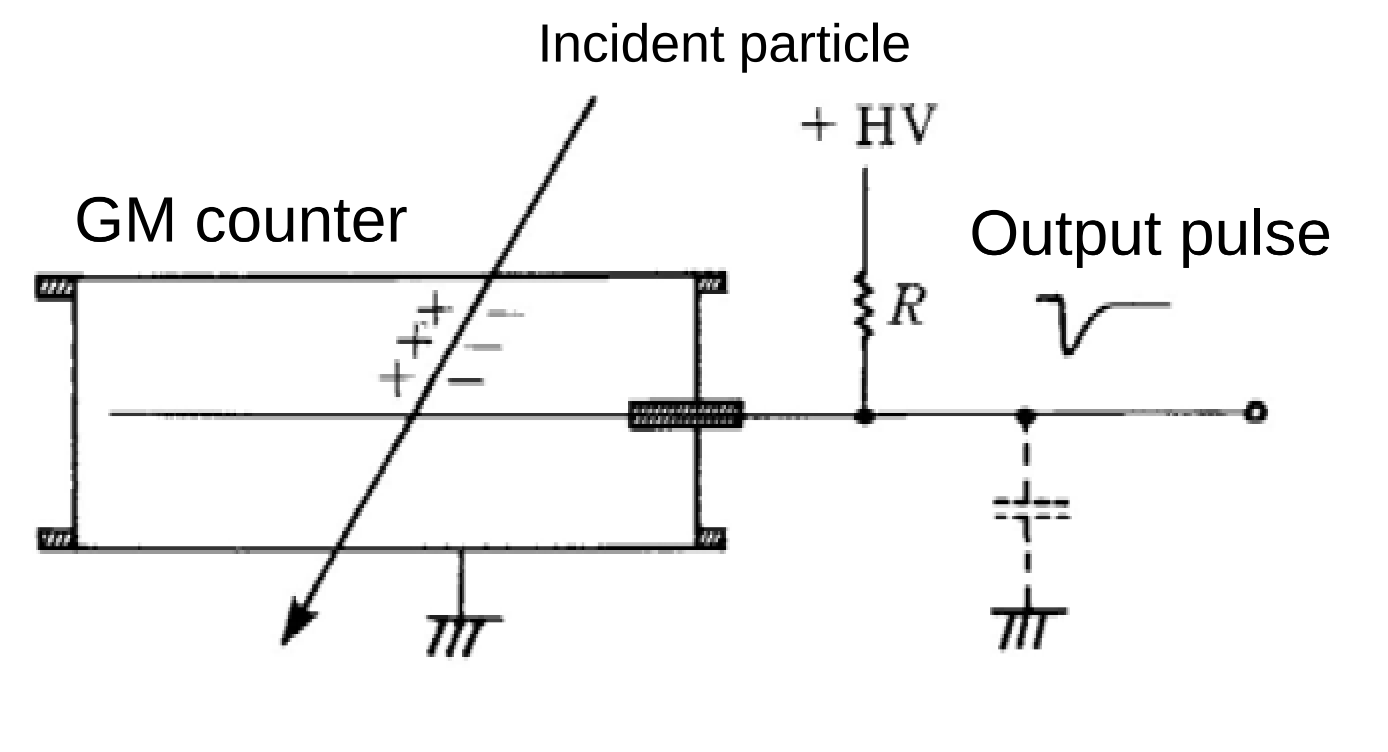

Self quenching type

Choice of gas

Little recombination for inert gas or nitrogen.

How does a recombination happen?

For Ion pair: e^- , X^+,

$e^- + X \rightarrow X^-$

$X^- + X^+ \rightarrow X + X$

Ramsauer effect:

Cross section of e-X+ reaction

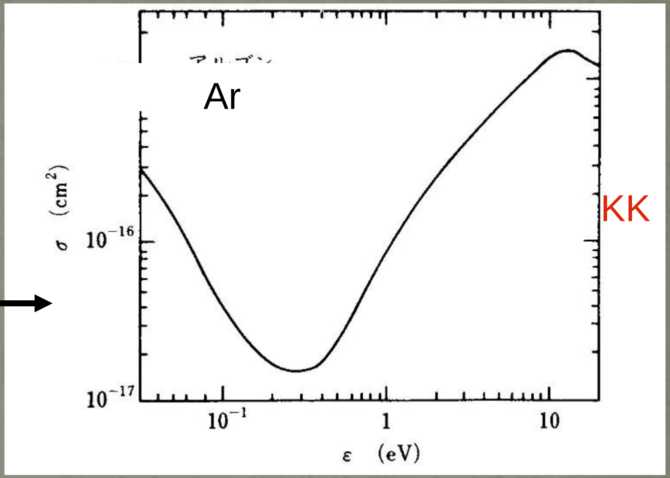

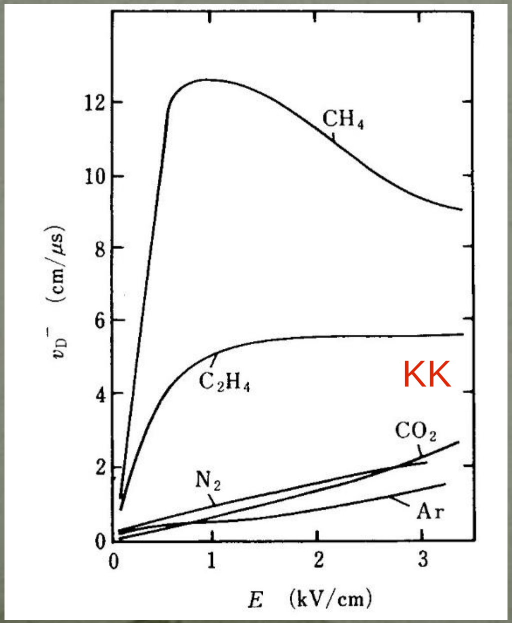

Gas mixture

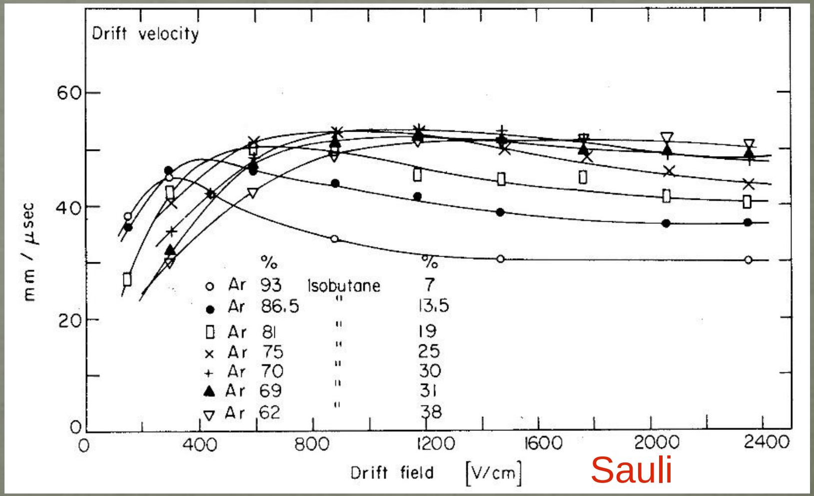

Drift velocity does not depend on the electric field

Examples

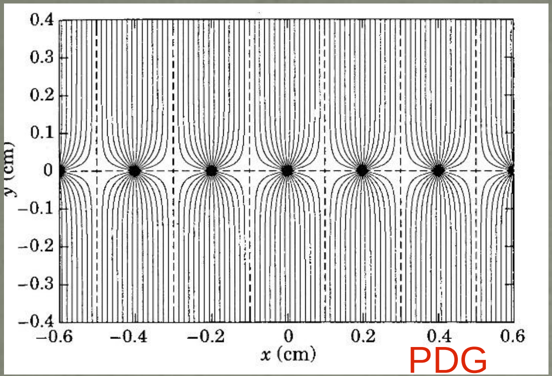

MWPC

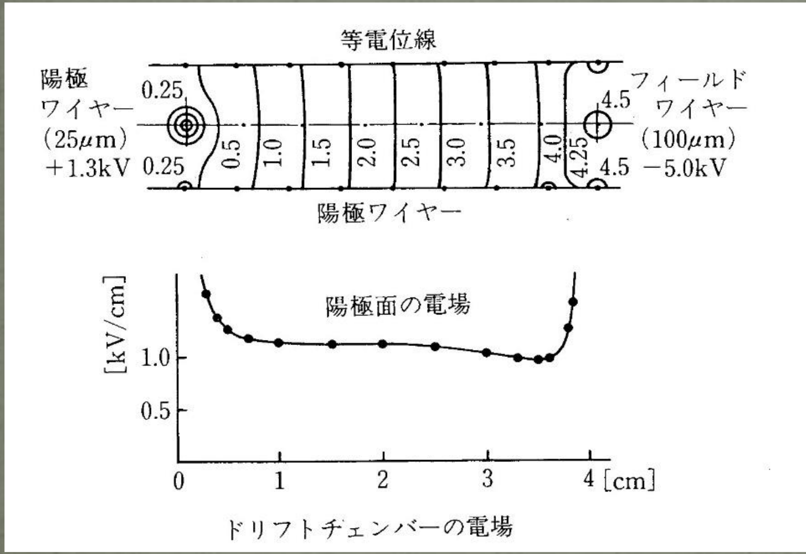

Drift chamber at early time

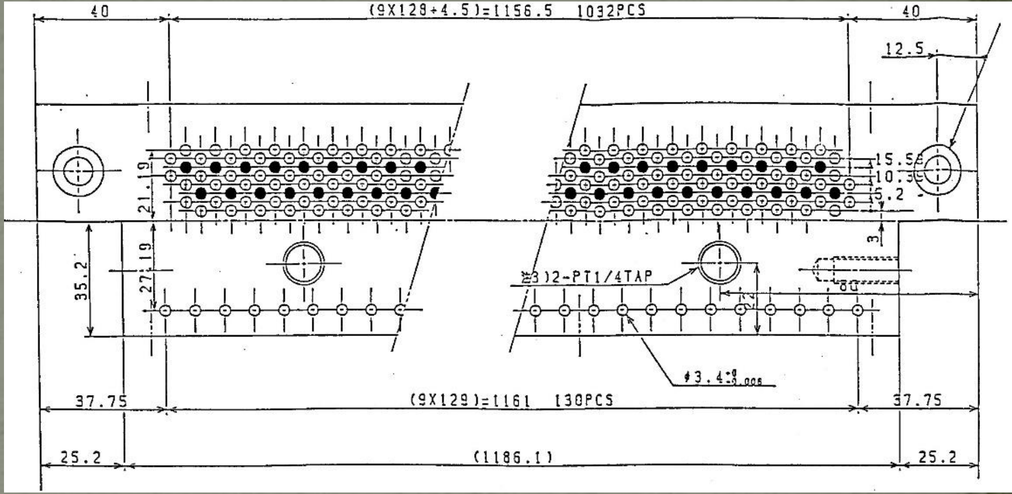

E137

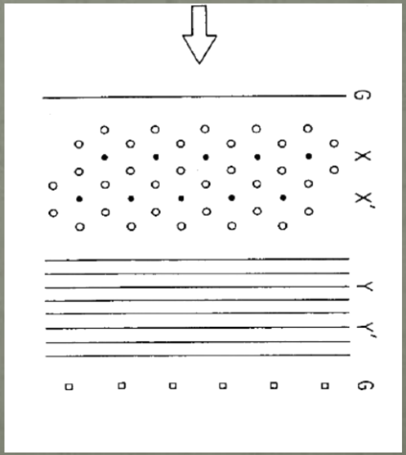

Problems

- Problems caused by slow movement of positive ions

  1． Long tail of the signal

  ⇒ Signal shaping is done with outside circuit

  2． Electric shield effect which causes a rate effect

  ⇒TPC with grid is an answer to these problems of positive ions.

- Problem caused by large size molecules of positive ions

  3． Aging : caused by adhering molecules to the cathode

  ⇒ Thick wire or flat sheet for cathode (prevent local adherence)

  ⇒ Mixing of quench gas: alcohol, ether, halogen-gas

- Limit of position resolution

  4． Determined by diffusion during drift of electrons

  $\gtrsim$ 100 μm

  inevitable effect because of gas filling

TPC

Fig. 3.18. Sketch of time projection chamber (TPC) for the PEP4 experiment [MA 78].

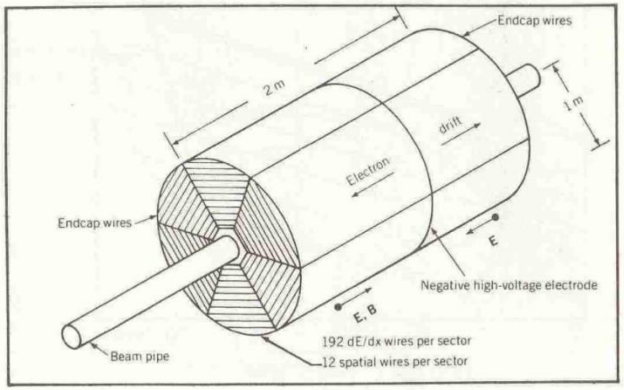

Fig. 3.19. Principle of track measurement by cathode pad readout in a TPC [FA 79].

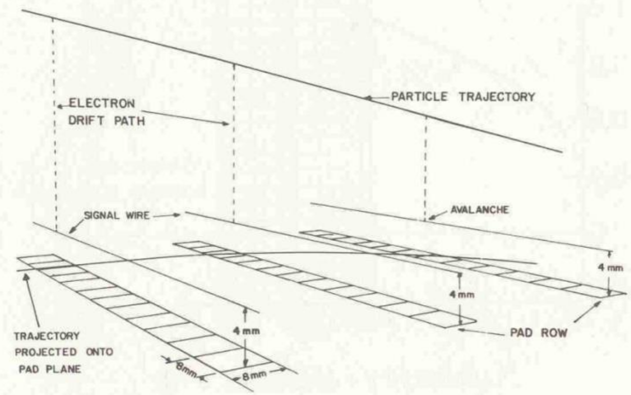

KK

- Measure the track in three dimensions by using sense-wire position, drift-time and cathode pads. 3d-readout
- Avoid a large positive-ion problem by narrowing the avalanche region near the sense wire. Reduce positive ion problem
- Minimize a diffusion by winding drift-electrons around a magnetic line of force. Reduce the diffusion effect

Ultimate gas chamber

TPC (cont)
Particle identification

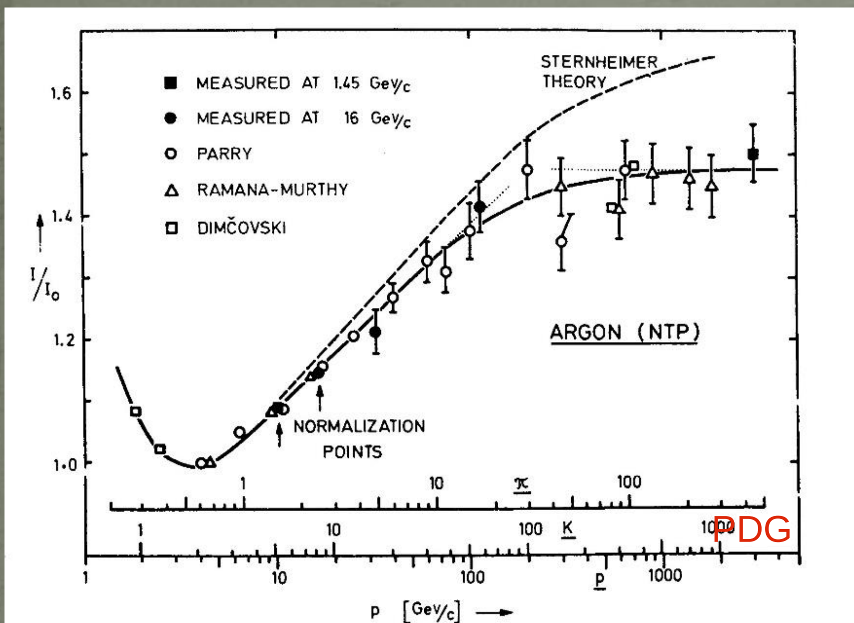

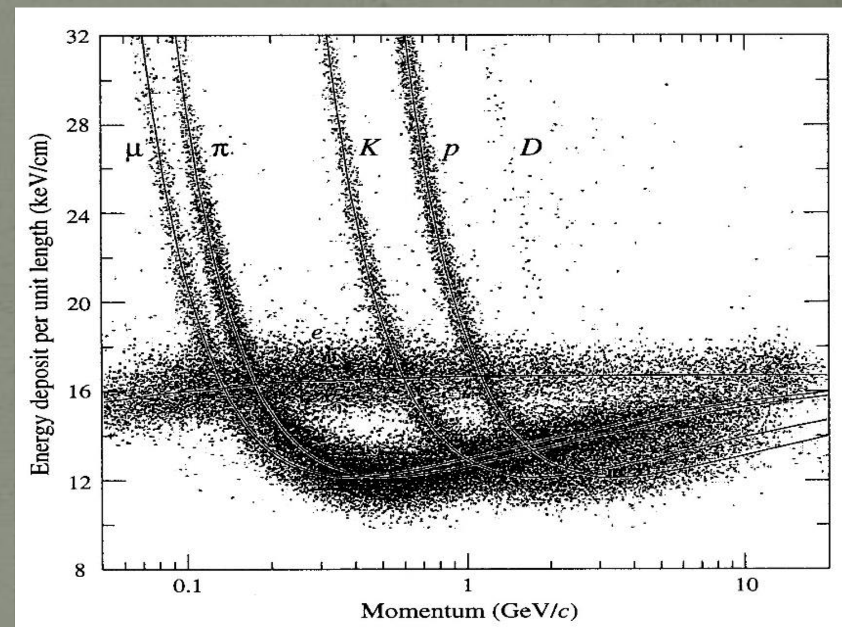

Semiconductor detector

Contents

- Properties of semiconductor
- p-n junction
- Reverse biasing
- Remarkable features

Properties of semiconductor

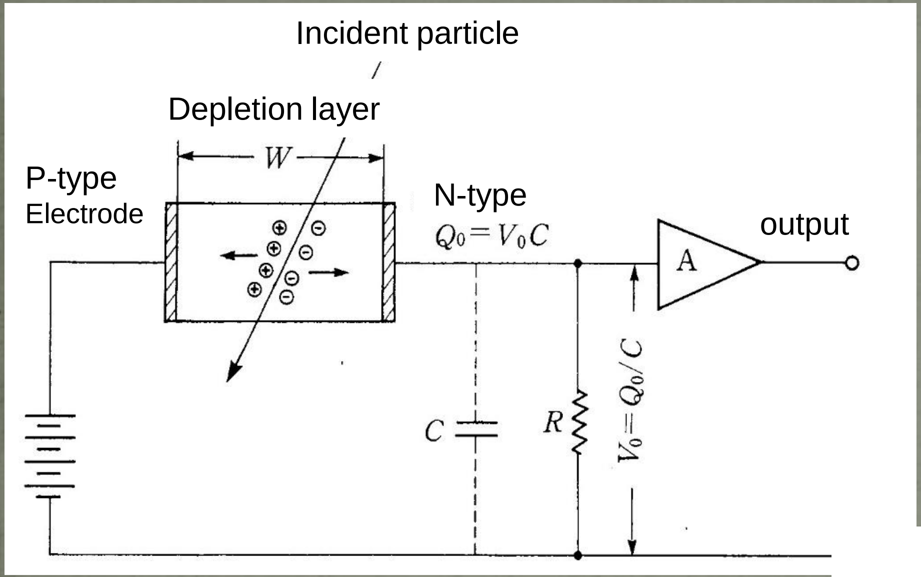

Energy levels of solid state

narrow gap between valence and conduction bands

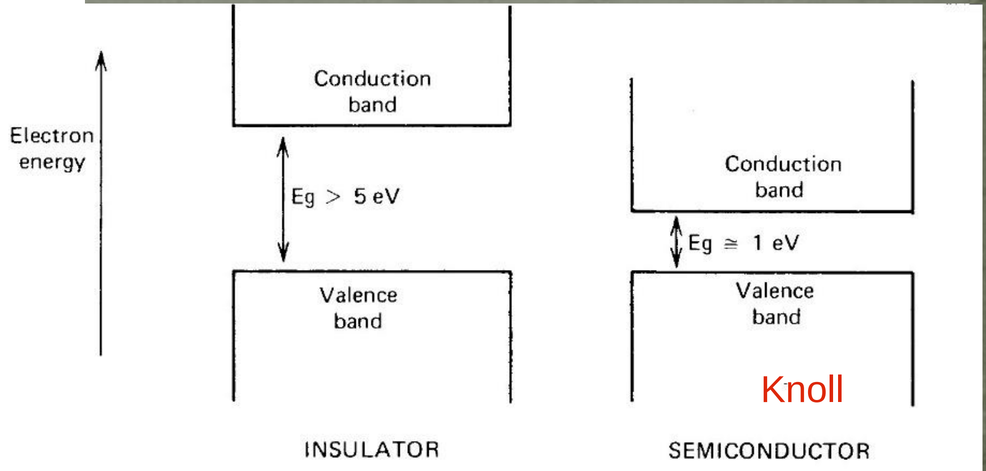

Same principle with a gas chamber (ionization chamber).

However, the carriers in solid state are electron and hole pairs in stead of free electron and positive ion pairs in gas.

How we can get high resistance ???

TABLE 11-1. Properties of Intrinsic Silicon and Germanium

	Si	Ge
Atomic number	14	32
Atomic weight	28.09	72.60
Stable isotope mass numbers	28-29-30	70-72-73-74-76
Density (300 K); g cm^{-3}	2.33	5.33
Atoms cm^{-3}	4.96×10^{22}	4.41×10^{22}
Dielectric constant	12	16
Forbidden energy gap (300 K); eV	1.115	0.665
Forbidden energy gap (0 K); eV	1.165	0.746
Intrinsic carrier density (300 K); cm^{-3}	1.5×10^{10}	2.4×10^{13}
Intrinsic resistivity (300 K); Ωcm	2.3×10^{5}	47
Electron mobility (300 K); cm^2/V-s	1350	3900
Hole mobility (300 K); cm^2/V-s	480	1900
Electron mobility (77 K); cm^2/V-s	2.1×10^{4}	3.6×10^{4}
Hole mobility (77 K); cm^2/V-s	1.1×10^{4}	4.2×10^{4}
Energy per hole-electron pair (300 K); eV	3.62	
Energy per hole-electron pair (77 K); eV	3.76	2.96
Fano factor (77 K)	0.143 (Ref. 7) 0.084 (Ref. 8) 0.085 to 0.137 (Ref. 12)	0.129 (Ref. 9) 0.08 (Ref. 10) $<$0.11 (Ref. 11) 0.057 0.064 (Ref. 12) 0.058 (Ref. 13)

From G. Bertolini and A. Coche, Eds., "Semiconductor Detectors," Elsevier-North Holland, Amsterdam (1968), except where noted.

Knoll

A pair can be produced by 3-4 eV energy. The density of solid state is higher than that of gas.

Seed will be much more than that of gas chamber, and amplification like gas amplification won't be necessary.

Small difference between velocities of electrons and hole unlike the gas case.

Still, high carrier density. How to realize no-carrier (higher resistance) world.

p-n junction

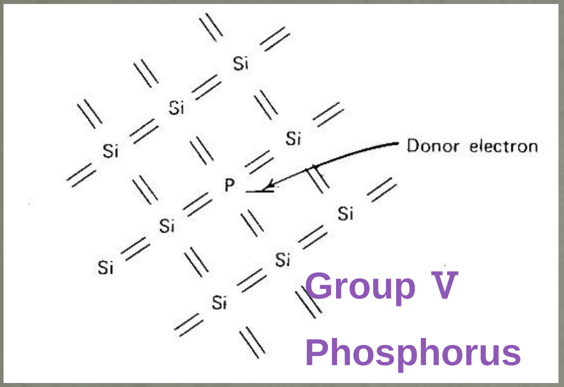

n-type silicon

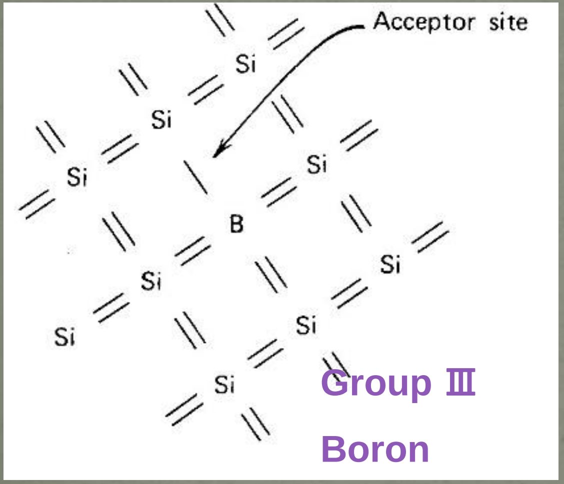

p-type silicon

Knoll

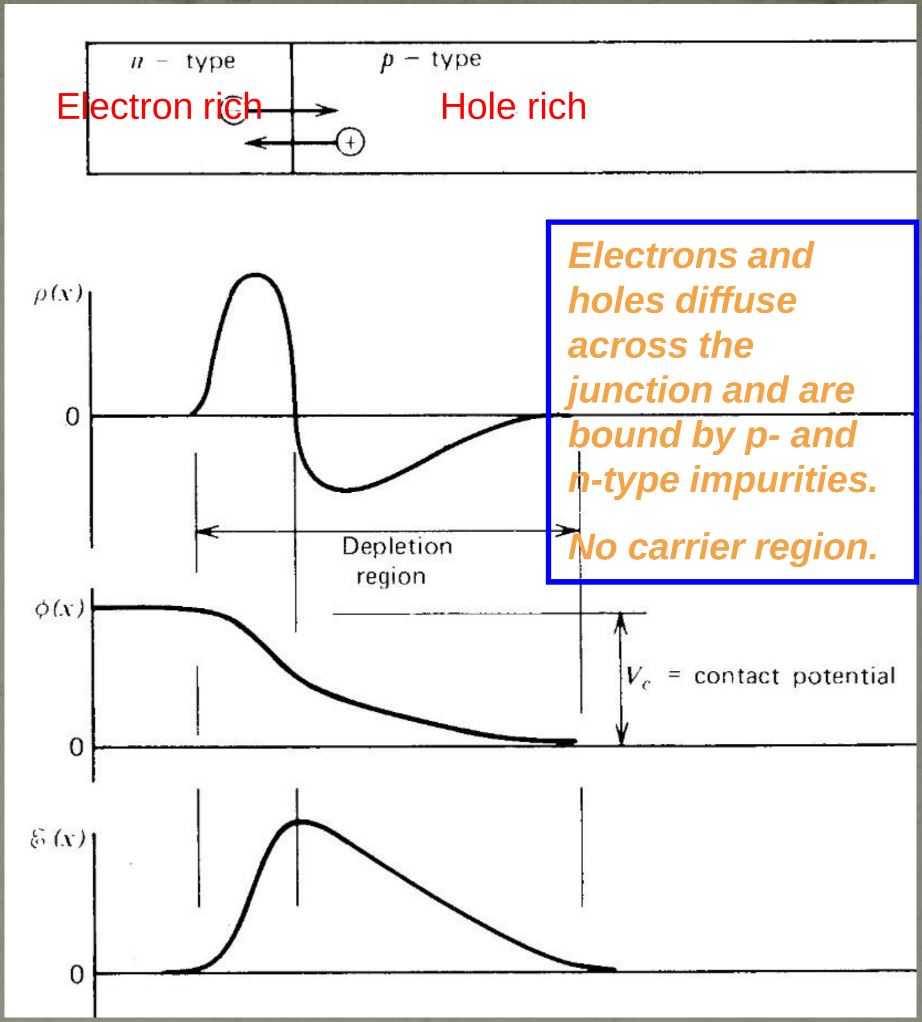

However,

V_C ≦ 1 V and thin depletion layer due to a space charge effect

Thin depletion layer →large capacitance (C) →small signal due to q/C

Reverse Biasing

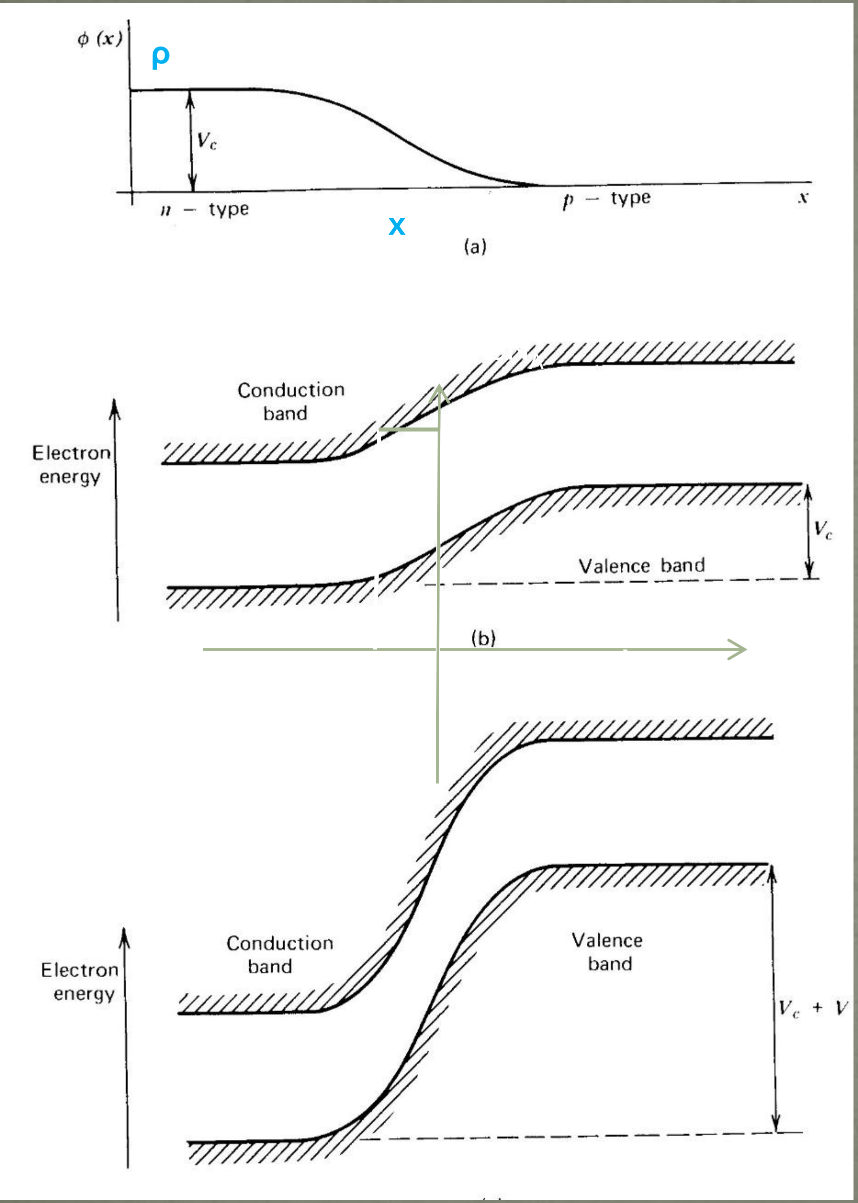

Knoll

Reverse biasing: supply of external voltage, in the reverse direction, which is the direction to increase the contact potential, expands the depletion layer.

To prevent discharge,

$E \leqq 10^6 – 10^7$ V/m

Simple model in one-dimension

Gauss's theorem: $\Delta \phi = -\rho / \varepsilon$

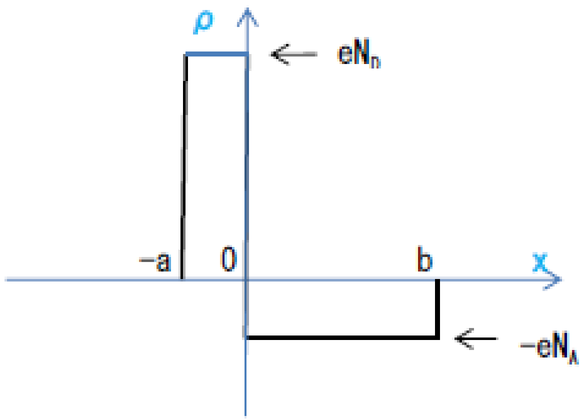

$d^2\phi/dx^2 = -eN_D/\varepsilon \quad (-a < x < 0)$

$= eN_A/\varepsilon \quad (0 < x < b)$

Boundary conditions

$d\phi/dx \,|_{x=-a,b} = 0$

$\phi(-a) = V, \ \phi(b) = 0$

ϕ for either side must match at $x = 0$

$N_D a = N_A b$

$a + b \equiv d, \ a \ll b \Rightarrow b \approx d, \ NA \equiv N$

Thickness of depletion layer: $d = [(2\varepsilon V)/(eN)]^{1/2}$

Capacitance: $C = \varepsilon/d = [(e\varepsilon N)/(2V)]^{1/2}$

Field strength: $E = V/d = [(eNV)/2\varepsilon)]^{1/2}$

Remarkable features of semiconductor detector

- Extremely good resolution of energy for low energy particles

Number of seed: $n = Ed / W$, where Ed and W are energy deposit and energy produce +/- pair

Ed is larger than gas due to higher density of solid by one thousand.

W is 3.62 eV for Si. It is very small.

Number of seed

semiconductor: $n = 10^6$

gas ： $n = 10^2$

plastic scintillator ： 10^3

crystal scintilator: 10^2

Best recode: Ge→0.054% for 8MeV γ、 0.71% 122keV γ

For this purpose, the thicker depletion layer is the better. Si-Li etc.

- Extremely good resolution of position for high energy particles

Large number of seeds with high density: RO from multi places

Small diffusion

Fine machining

Moreover, response is fast, due to thin layer of depletion and fast movement of hole.

Silicon Vertex detector is now a crucial detector for flavor tagging.

Fig. 3.34. Cross-section of silicon microstrip detector with capacitive charge division [HY 83].

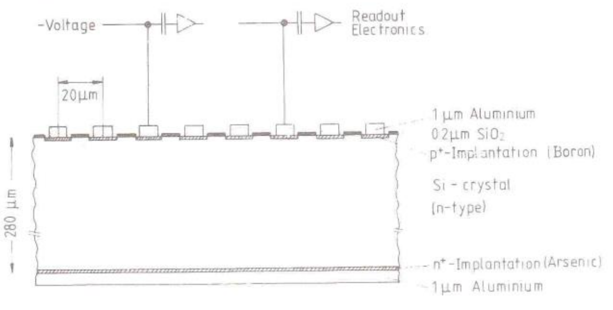

Position is obtained from the measurement of induced current on the electrode (strip, pixel) . Highly-dense seed of electron-holes is crucial .

Table 35.1: Typical resolutions and deadtimes of common charged particle detectors. Revised November 2011.

Detector Type	Intrinsinc Spatial Resolution (rms)	Time Resolution	Dead Time
Resistive plate chamber	$\lesssim 10$ mm	1 ns (50 ps[a])	—
Streamer chamber	300 μm[b]	2 μs	100 ms
Liquid argon drift [7]	~175–450 μm	~ 200 ns	~ 2 μs
Scintillation tracker	~100 μm	100 ps/n[c]	10 ns
Bubble chamber	10–150 μm	1 ms	50 ms[d]
Proportional chamber	50–100 μm[e]	2 ns	20-200 ns
Drift chamber	50–100 μm	2 ns[f]	20-100 ns
Micro-pattern gas detectors	30–40 μm	$<$ 10 ns	10-100 ns
Silicon strip	pitch/(3 to 7)[g]	few ns[h]	$\lesssim 50$ ns[h]
Silicon pixel	$\lesssim 10$ μm	few ns[h]	$\lesssim 50$ ns[h]
Emulsion	1 μm	—	—

B meson tagging $\tau(B^+) \sim 1.6 \times 10^{-12}$ sec, $\tau(B^0) \sim 1.5 \times 10^{-12}$ sec
$c\tau \sim 450$ μm

Belle II Detector

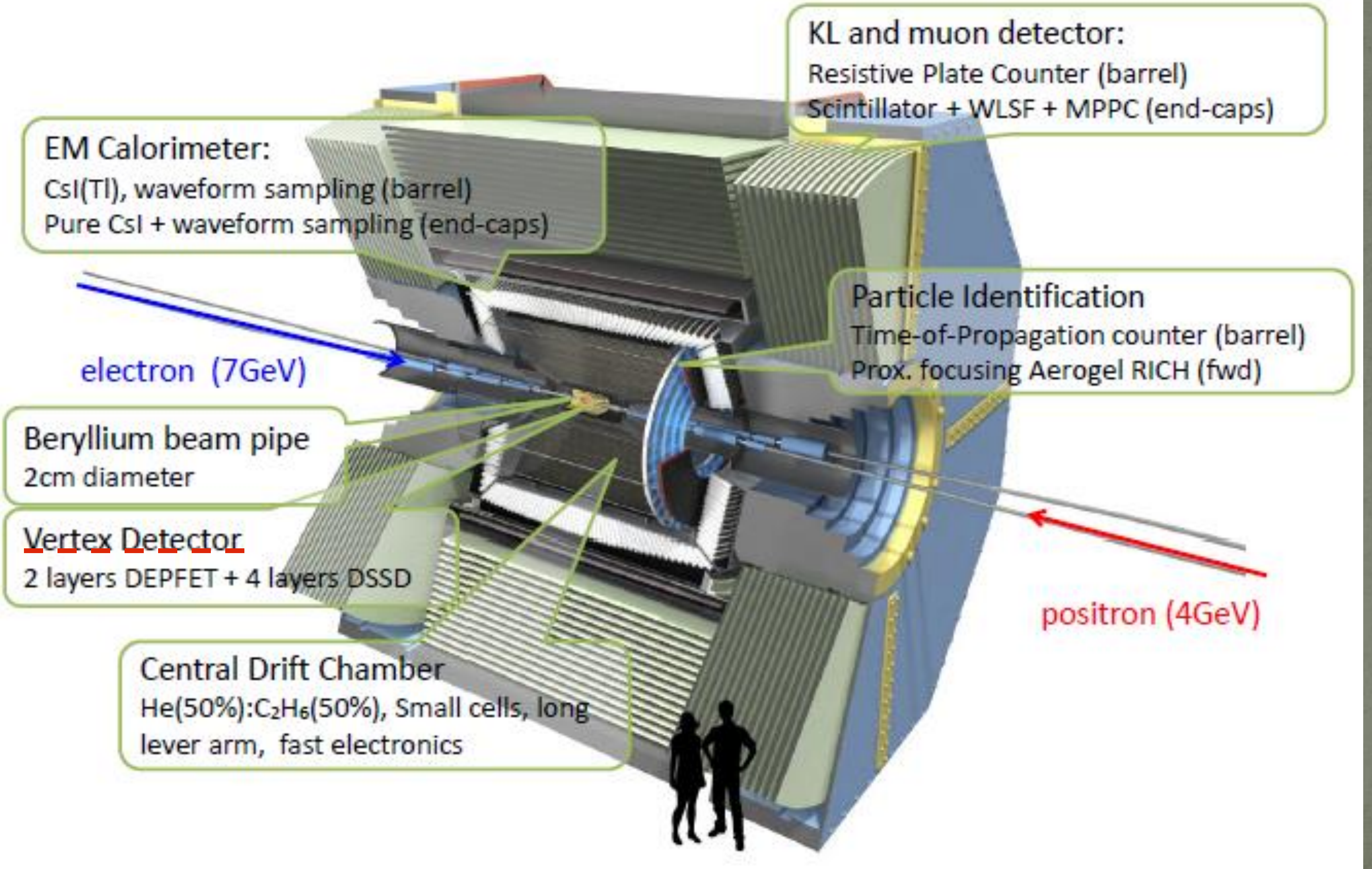

LHC-Atlas

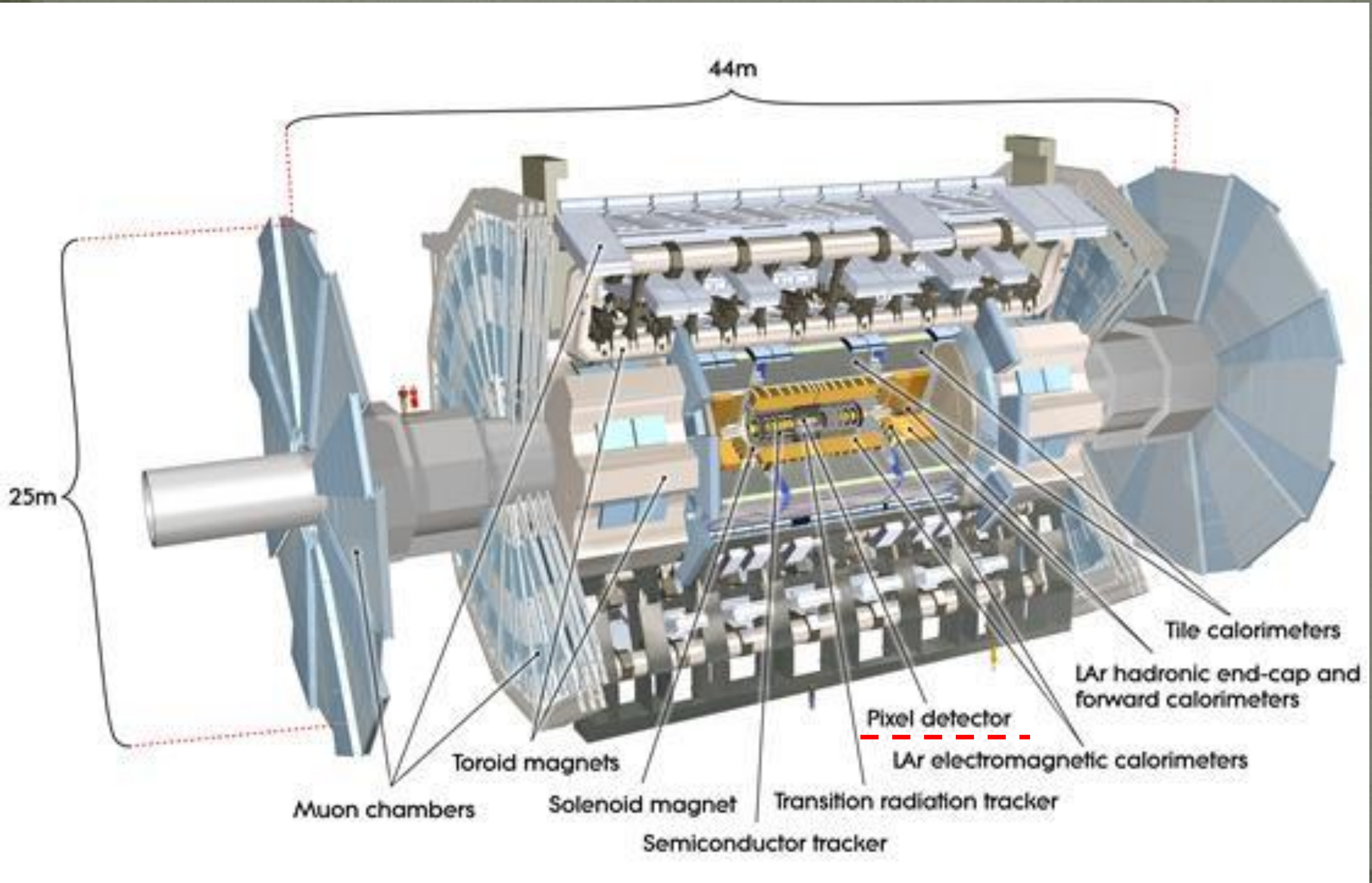

44m
25m
Tile calorimeters
LAr hadronic end-cap and forward calorimeters
Pixel detector
LAr electromagnetic calorimeters
Toroid magnets
Muon chambers
Solenoid magnet
Transition radiation tracker
Semiconductor tracker

dE/dx measurement

Detector using light

Plastic scintillator

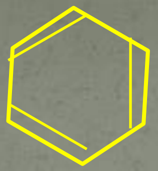

Energy levels of an organic molecule with π-electron structure (phenyl)

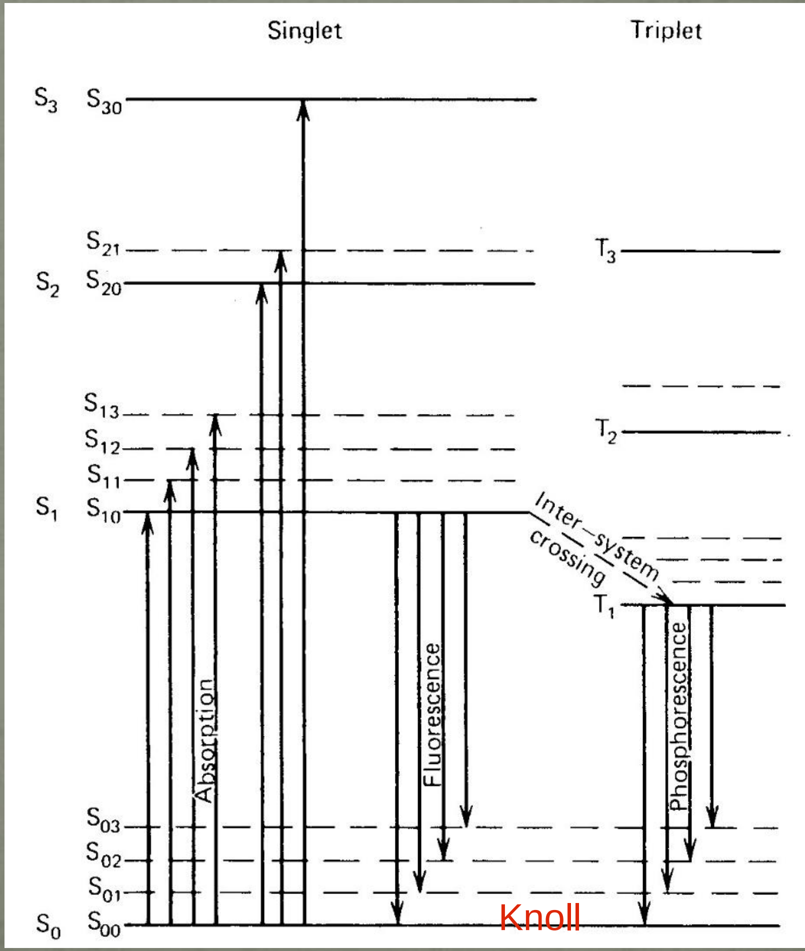

S0-S1: 3 – 4 eV

S00-S01: 0.15 eV > 0.025 eV
Most of electrons stays at S00 (ground state)

Sij: vibrational states, transitions inside {S0} and {S1}, Sij →Si0, are radiationless, and their decay times are:

τ{S10}：nsec, τ{T1}: msec

Another route to the ground state

T1 + T1 →S1 +S0

This is useful for PID, n/γ separation.

PVT; poly-vinyl-toluene

PS； poly-styrene

Liquid scintillators; xylene, etc

Wave length shift to visible light for better transmission

PDG

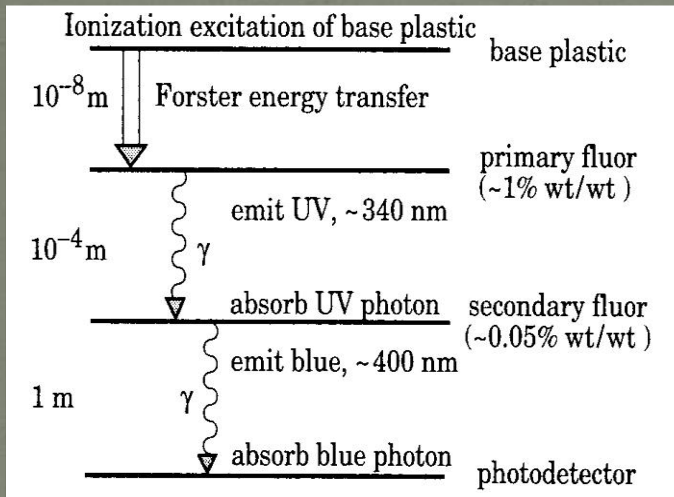

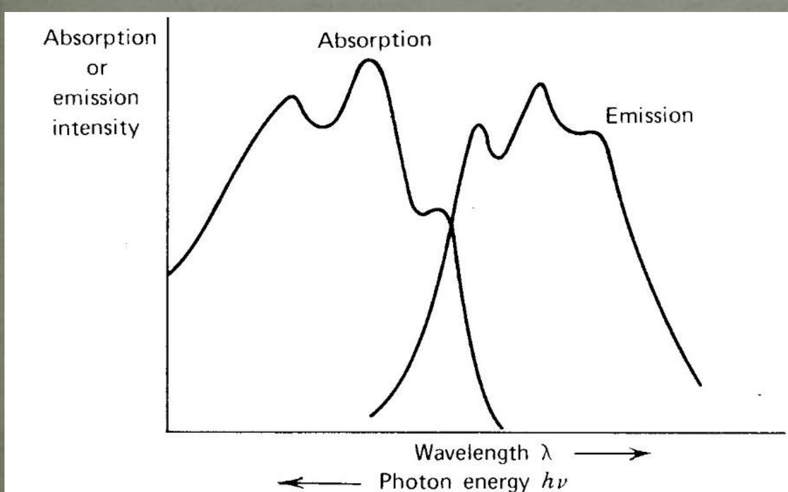

Knoll

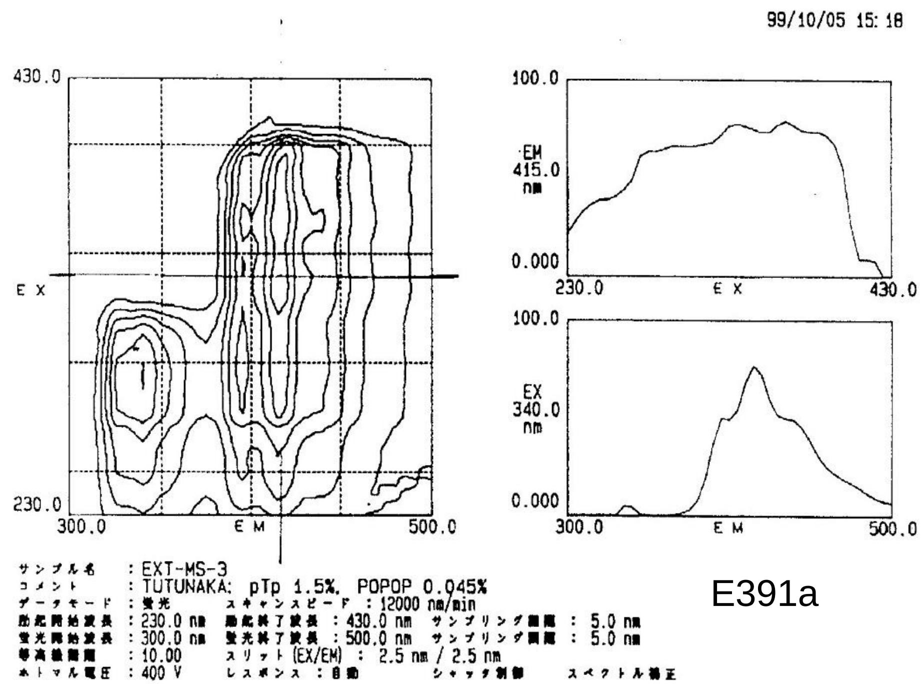

E391a

Fig. 2.4: 押し出し成形法で製造したMS樹脂シンチレーター（PTP 1.5% + POPOP 0.045）の励起発光スペクトル。Fluorescence Spectrometer HITACHI F-4500を用いて測定した。左図は2次元の励起発光スペクトルで，横軸は発光波長，縦軸は吸光（励起）波長である。右上図は発光波長410nmに対する励起波長スペクトル，右下図は励起波長340nmに対する発光波長スペクトルである。

Readout method

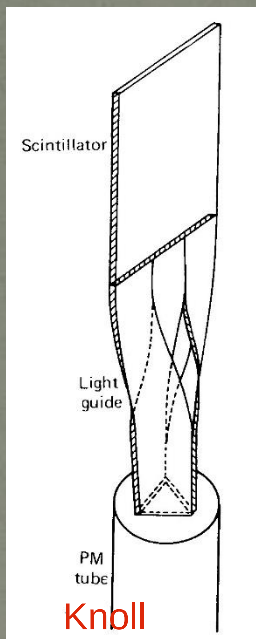

Knoll

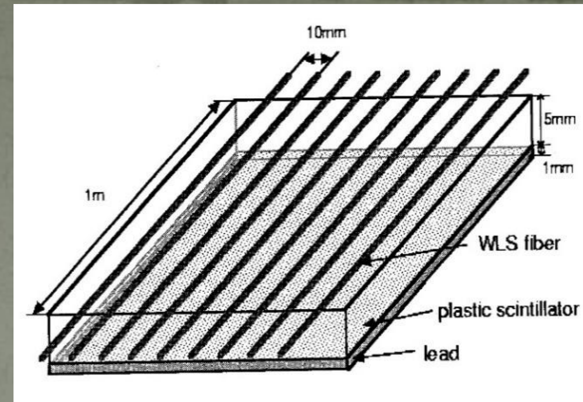

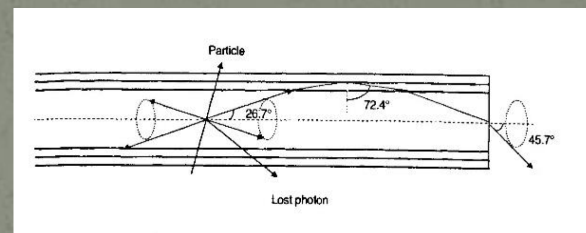

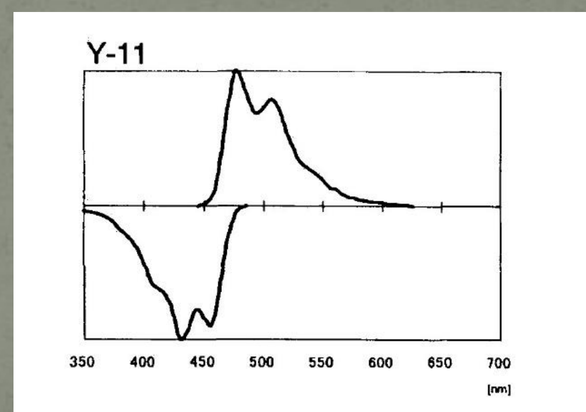

Clad structure

Through light guide

(direct RO)

Through WLS-fibers

Attenuation is smaller than that of the direct RO at a long distance. We can reduce the area of photo cathode.

Inorganic (Crystal) scintillators

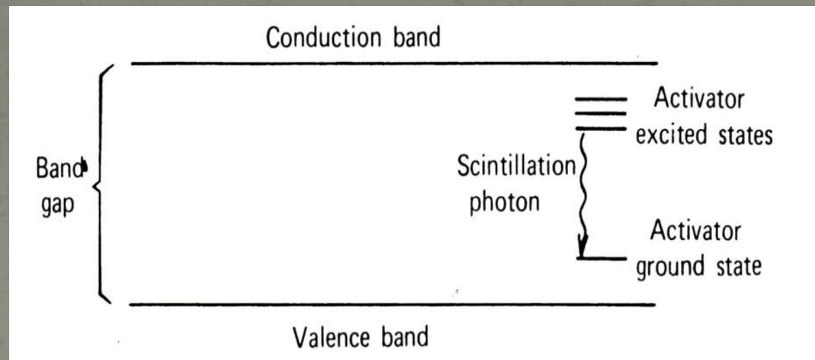

Knoll

Table 28.2: Properties of several inorganic crystal scintillators. Most of the notation is defined in Sec. 6 of this *Review*.

Parameter:	ρ	MP	X_0	R_M	dE/dx	λ_I	τ_{decay}	λ_{max}	n^*	Relative output†	Hygro-scopic?	$d(LY)/dT$
Units:	g/cm^3	°C	cm	cm	MeV/cm	cm	ns	nm				%/°C‡
NaI(Tl)	3.67	651	2.59	4.8	4.8	41.4	230	410	1.85	100	yes	$\sim$0
BGO	7.13	1050	1.12	2.3	9.0	21.8	300	480	2.15	9	no	-1.6
BaF_2	4.89	1280	2.06	3.4	6.6	29.9	630^s	300^s	1.50	21^s	no	-2^s
							0.9^f	220^f		2.7^f		$\sim 0^f$
CsI(Tl)	4.51	621	1.85	3.5	5.6	37.0	1300	560	1.79	45	slight	0.3
CsI(pure)	4.51	621	1.85	3.5	5.6	37.0	35^s	420^s	1.95	5.6^s	slight	-0.6
							6^f	310^f		2.3^f		
$PbWO_4$	8.3	1123	0.9	2.0	10.2	18	50^s	560^s	2.20	0.1^s	no	-1.9
								10^f	420^f		0.6^f	
LSO(Ce)	7.40	2070	1.14	2.3	9.6	21	40	420	1.82	75	no	-0.3
GSO(Ce)	6.71	1950	1.37	2.4	8.9	22	600^s	430	1.85	3^s	no	-0.1
							56^f			30^f		

PDG

Other source of light : Cherenkov light

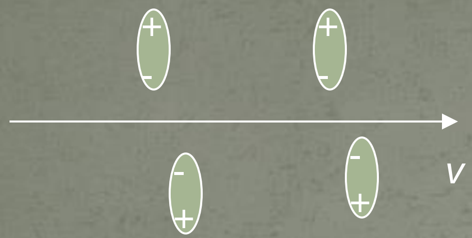

A particle cause polarization and the polarization returns to the state before. Very tiny, but coherence enhance the emission of light.

material	Refractive index (n)	Critical energy (E_c, MeV)			Emission angle θ_0 (degree, for β=1)
		proton	μ-on	electron	
Air	1.000284	38.5×10^3	4.3×103	61	1.4
water	1.34	450	50	0.25	42
Lucite	1.50	310	35	0.17	48
Lead glass	1.68	220	26	0.13	54

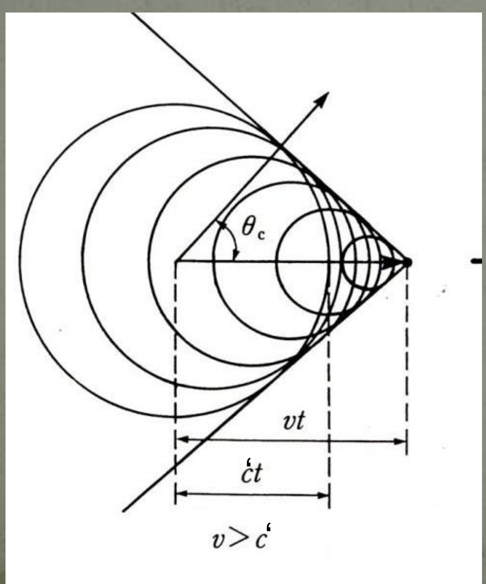

$c' = c / n$

$\cos\theta_c = v/c'$

$= 1/n\beta$

Critical energy:

$n\beta > 1$, $\beta_c = 1/n$

$E_c = (\gamma_c - 1)m$,

Emission angle

$\cos\theta_c > 1/n$

$\theta_c < \theta_0$

$= \cos^{-1}(1/n)$

Light yield ： $d^2N/dxd\lambda = 2\pi\alpha z^2 \sin^2\theta/\lambda^2$

When electrons and protons of 2 GeV/c run through water, the emission angles are 41.25°, 33.84°,respectively. We can measure the particle direction

$dN/dx = 99.6,\ 71.0\ cm^{-1}$; λ= 400-500 nm

Transition radiation

$N \propto \gamma$

Photo-sensor
Photo-Multiplier-Tube（PMT)

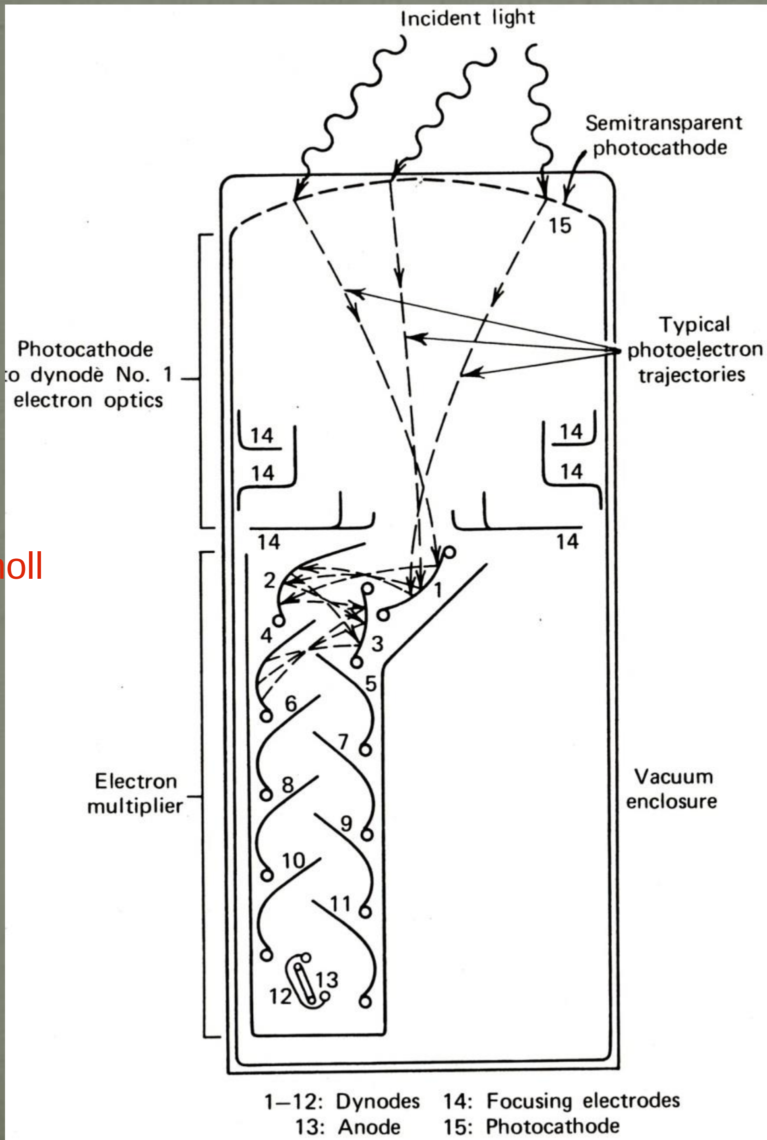

Knoll

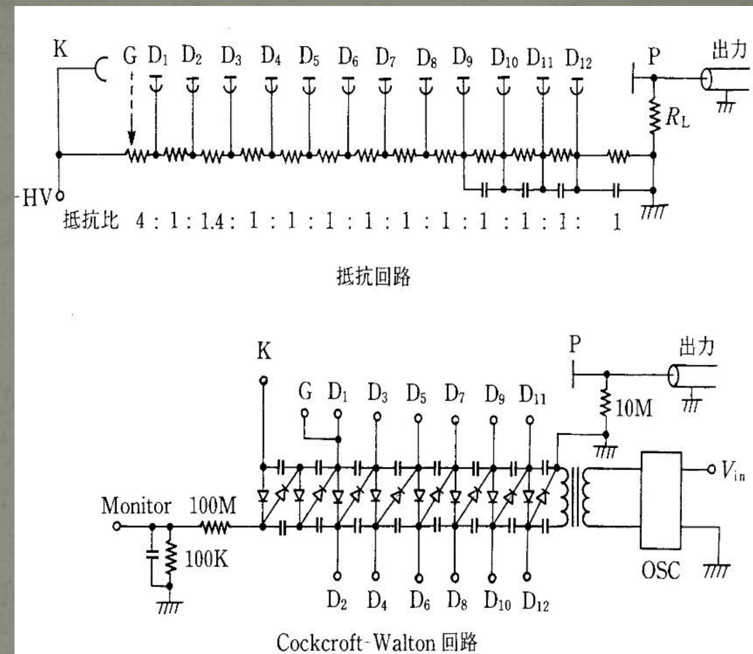

Hamamatsu R329 高圧回路

3・27 図 光電子増倍管の高電圧回路

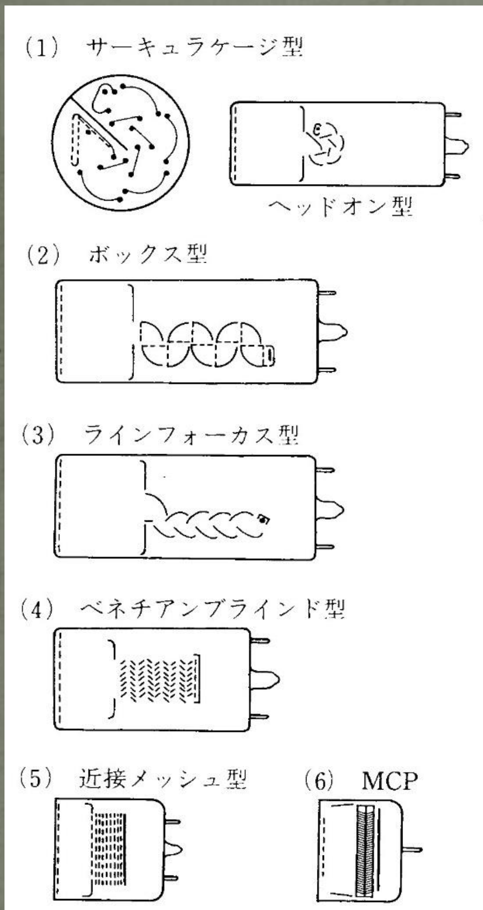

Cathode

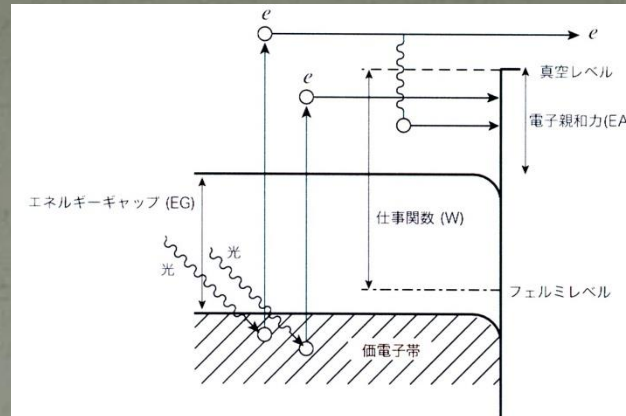

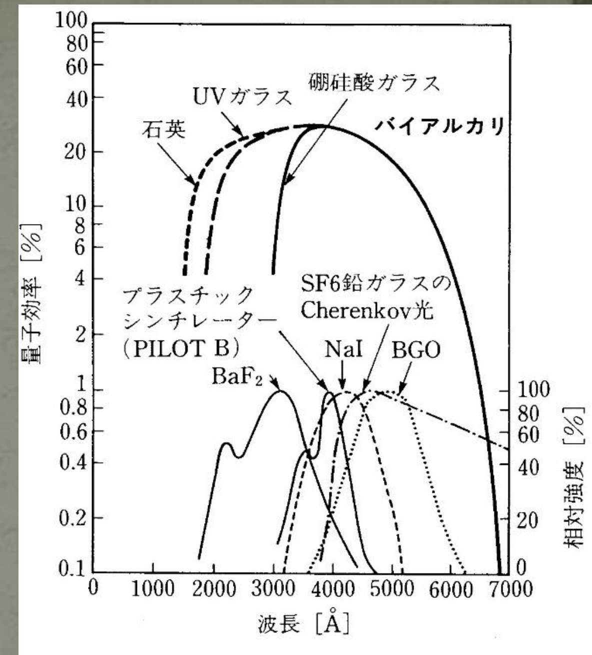

Na / K / Rb / Cs +Sb

Dinode

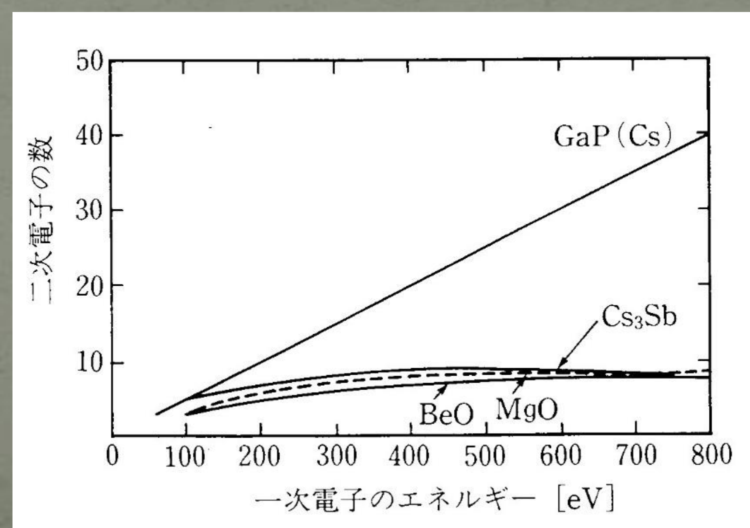

Various photodetectors

Table 35.2: Representative characteristics of some photodetectors commonly used in particle physics. The time resolution of the devices listed here vary in the 10–2000 ps range.

Type	λ (nm)	$\epsilon_Q\,\epsilon_C$	Gain	Risetime (ns)	Area (mm^2)	1-p.e noise (Hz)	HV (V)	Price (USD)
PMT*	115–1700	0.15–0.25	10^3–10^7	0.7–10	10^2–10^5	10–10^4	500–3000	100–5000
MCP*	100–650	0.01–0.10	10^3–10^7	0.15–0.3	10^2–10^4	0.1–200	500–3500	10–6000
HPD*	115–850	0.1–0.3	10^3–10^4	7	10^2–10^5	10–10^3	$\sim 2 \times 10^4$	~600
GPM*	115–500	0.15–0.3	10^3–10^6	$O(0.1)$	$O(10)$	10–10^3	300–2000	$O(10)$
APD	300–1700	~0.7	10–10^8	$O(1)$	10–10^3	1–10^3	400–1400	$O(100)$
PPD	320–900	0.15–0.3	10^5–10^6	~ 1	1–10	$O(10^6)$	30–60	$O(100)$
VLPC	500–600	~0.9	$\sim 5 \times 10^4$	~ 10	1	$O(10^4)$	~7	~1

PMT: Photomultiplier tube, MCP: Microchannel plate, HPD: Hybrid photon detector

GPM: Gaseous photon detector, APD: Avalanche photo diode,

PPD: Pixelized photon detector, VLPC: Visible light photon couter

R&D in the E391a experiment

- **Scintillator : Extruded MS-resin**

  Among three method to make plastic sheet, cast, injection-mold, and extrusion,

  extrusion is only method which has no limit in length, possible to use MS, which is mechanically strong, cheap for mass-production.

- **PMT : EGP**

  Optimized for green light (WLSF)

  improved quantum efficiency at 500 nm.

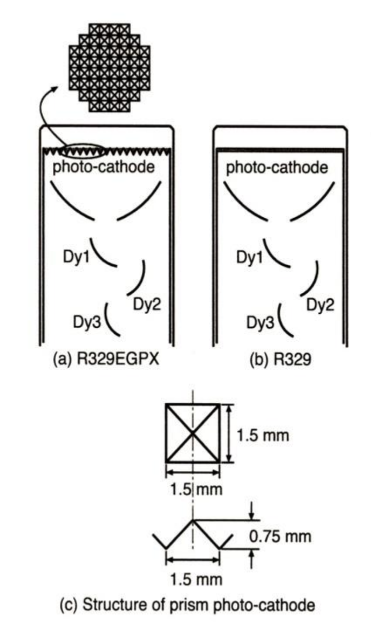

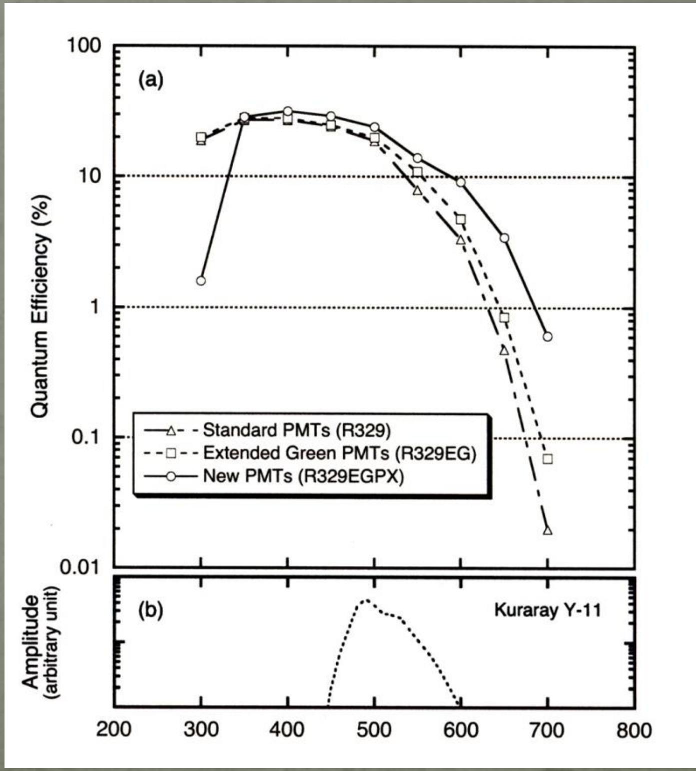

Electromagnetic calorimeters
for an energy measurement of photons and electrons

Table 28.5: Resolution of typical electromagnetic calorimeters. E is in GeV.

Technology (Experiment)	Depth	Energy resolution	Date
NaI(Tl) (Crystal Ball)	$20X_0$	$2.7\%/E^{1/4}$	1983
$Bi_4Ge_3O_{12}$ (BGO) (L3)	$22X_0$	$2\%/\sqrt{E} \oplus 0.7\%$	1993
CsI (KTeV)	$27X_0$	$2\%/\sqrt{E} \oplus 0.45\%$	1996
CsI(Tl) (BaBar)	16–$18X_0$	$2.3\%/E^{1/4} \oplus 1.4\%$	1999
CsI(Tl) (BELLE)	$16X_0$	1.7% for $E_\gamma > 3.5$ GeV	1998
$PbWO_4$ (PWO) (CMS)	$25X_0$	$3\%/\sqrt{E} \oplus 0.5\% \oplus 0.2/E$	1997
Lead glass (OPAL)	$20.5X_0$	$5\%/\sqrt{E}$	1990
Liquid Kr (NA48)	$27X_0$	$3.2\%/\sqrt{E} \oplus 0.42\% \oplus 0.09/E$	1998
Scintillator/depleted U (ZEUS)	20–$30X_0$	$18\%/\sqrt{E}$	1988
Scintillator/Pb (CDF)	$18X_0$	$13.5\%/\sqrt{E}$	1988
Scintillator fiber/Pb spaghetti (KLOE)	$15X_0$	$5.7\%/\sqrt{E} \oplus 0.6\%$	1995
Liquid Ar/Pb (NA31)	$27X_0$	$7.5\%/\sqrt{E} \oplus 0.5\% \oplus 0.1/E$	1988
Liquid Ar/Pb (SLD)	$21X_0$	$8\%/\sqrt{E}$	1993
Liquid Ar/Pb (H1)	20–$30X_0$	$12\%/\sqrt{E} \oplus 1\%$	1998
Liquid Ar/depl. U (DØ)	$20.5X_0$	$16\%/\sqrt{E} \oplus 0.3\% \oplus 0.3/E$	1993
Liquid Ar/Pb accordion (ATLAS)	$25X_0$	$10\%/\sqrt{E} \oplus 0.4\% \oplus 0.3/E$	1996

PDG

Similar features for hadron calorimeter

Decomposition of energy resolution

$\Delta E/E = C_1/\sqrt{E} + C_2 + C_3 / E$; just an empirical formula, but convinient

S: signal from the calorimeter
Total absorption type detector ≡ S ∞ E ; E = a·S ; proportionality

C_1 term : main term of resolution.
A particle looses its energy through an ionization process along charged tracks, and the ionization energy will be converted to an electronic signal. In the case of PMT readout, the smallest number, which makes the largest statistical fluctuation through this processing, is number of photo-electron, N_{pe}, before the large electron multiplication in PMT tube. E is proportional to N_{pe} and the error ΔE fluctuates as $\sqrt{N_{pe}}$, then $\Delta E/E \propto 1/\sqrt{N_{pe}} \propto 1/\sqrt{E}$.
It is similar with other readout . In the case of sampling calorimeter, consisting of active and non-active layers, the fluctuation of the sampling is also proportional to $\sqrt{E}$.

C_2 term: ΔE ∞ E ; Just as an ambiguity of calibration of the coefficient of a linear function.

C_3 term ; ΔE is energy-independent like a fluctuation given by electoric noise at the measurement.

For the ideal condition, noiseless operation and perfect calibration, the resolution is uniquely determined by C_1 term.

5. Examples and discussions

- 5.1 Spectrometer

  Momentum measurement by a magnetic spectrometer is better for low energy particles, while at high energy a calorimeter can measure the particle energy with a better resolution than at low energy.

Momentum measurement

Combination of a magnetic field and the track measurement

Particle motion in the magnetic field

Lorentz force $d\mathbf{p}/dt = q(\mathbf{v} \times \mathbf{B})$;MKSA （Coulomb、Volt、Tesla）

; just change the direction no gain of energy

For B ⊥ v $p\, d\theta/dt = q\, v\, B$

$\rho\omega = v$

$f = 2\pi/\omega$;

Cyclotron frequency

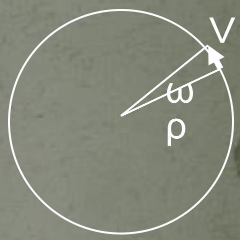

Non-relativistic	Relativistic
$p = mv$	$p = mv\gamma$
$d\theta/dt \equiv \omega = qB/m$	$\omega = qB/m\gamma$
(Energy independent)	(Energy dependent)

$\rho = v/\omega = mv/qB = p/qB$ $\rho = v/\omega = mv\gamma/qB = p/qB$; Same equation !!

p = 03Bρ, for q=e, where [p] = GeV/c, [B] = Tesla and [ρ] = m

Magnet depth: L $\rho\sin\theta = L$

$p = 0.3BL / \sin\theta$

$\mathbf{dp/p = (p / 0.3BL)\, d\theta}$ **:**

$= 3\times10^{-3}\, p$;for BL=1 Tm, dθ= 1 mradian

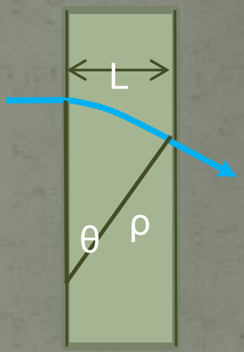

Resolution is proportional to momentum; worse at the higher energy!!

Clear contrast with calorimeter: resolution shows $1/\sqrt{E}$ dependence

Magnetic spectrometer of E137

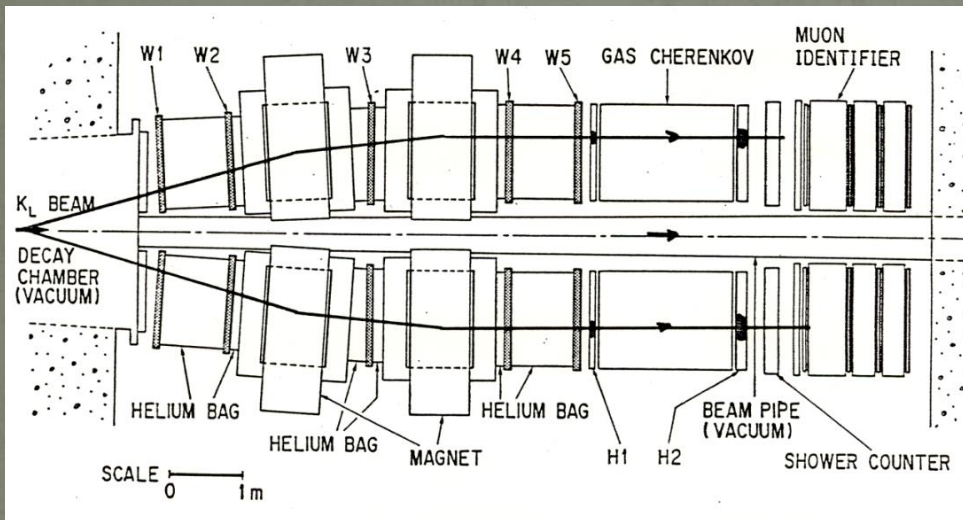

$p = 0.3BL / \sin\theta$
$P\sin\theta = P_T = 0.3BL$; magnet gives P_T kick

By setting magnetic field around 220 MeV/c kick, we can remove most of three-body decays and select four two-body decays with almost equal efficiency by the parallel trigger at downstream. The four modes were collected simultaneously.

This is true for KL decay at beam axis of any energy.

Such a simple trigger is possible due to low energy of larger opening angle.

Two body decay in KL rest frame

P_{CM}

In laboratory frame

P_{CM} (KL→ππ, μμ, μe, ee) =206, 225, 238, 249 MeV/c

We also achieved similar mass resolution with the BNL competitor with less DC position resolution of 300 μm. They have to operate DC at 150 μm.
We can operate DC at low voltage. It brought us a big margin in high-rate enviroment.

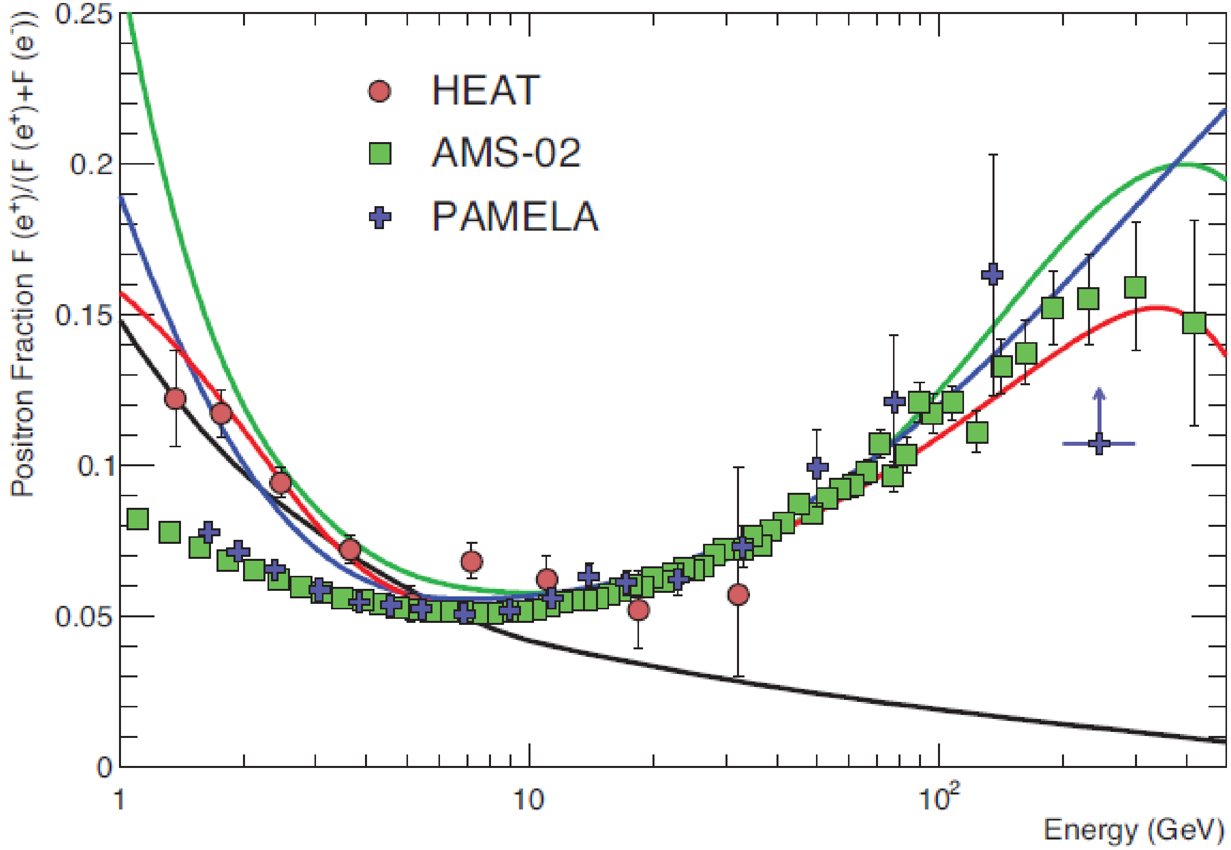

Figure 30.3: The positron fraction (ratio of the flux of e^+ to the total flux of e^+ and e^-) [26,24,30]. The heavy black line is a model of pure secondary production [28] and the three thin lines show three representative attempts to model the positron excess with different phenomena: green: dark matter decay [29]; blue: propagation physics [32]; red: production in pulsars [40]. The ratio below 10 GeV is dependent on the polarity of the solar magnetic field.

AMS could not deliver a super conducting magnet to the ISS

Examples and discussions

ν detectors

Super Kamiokande

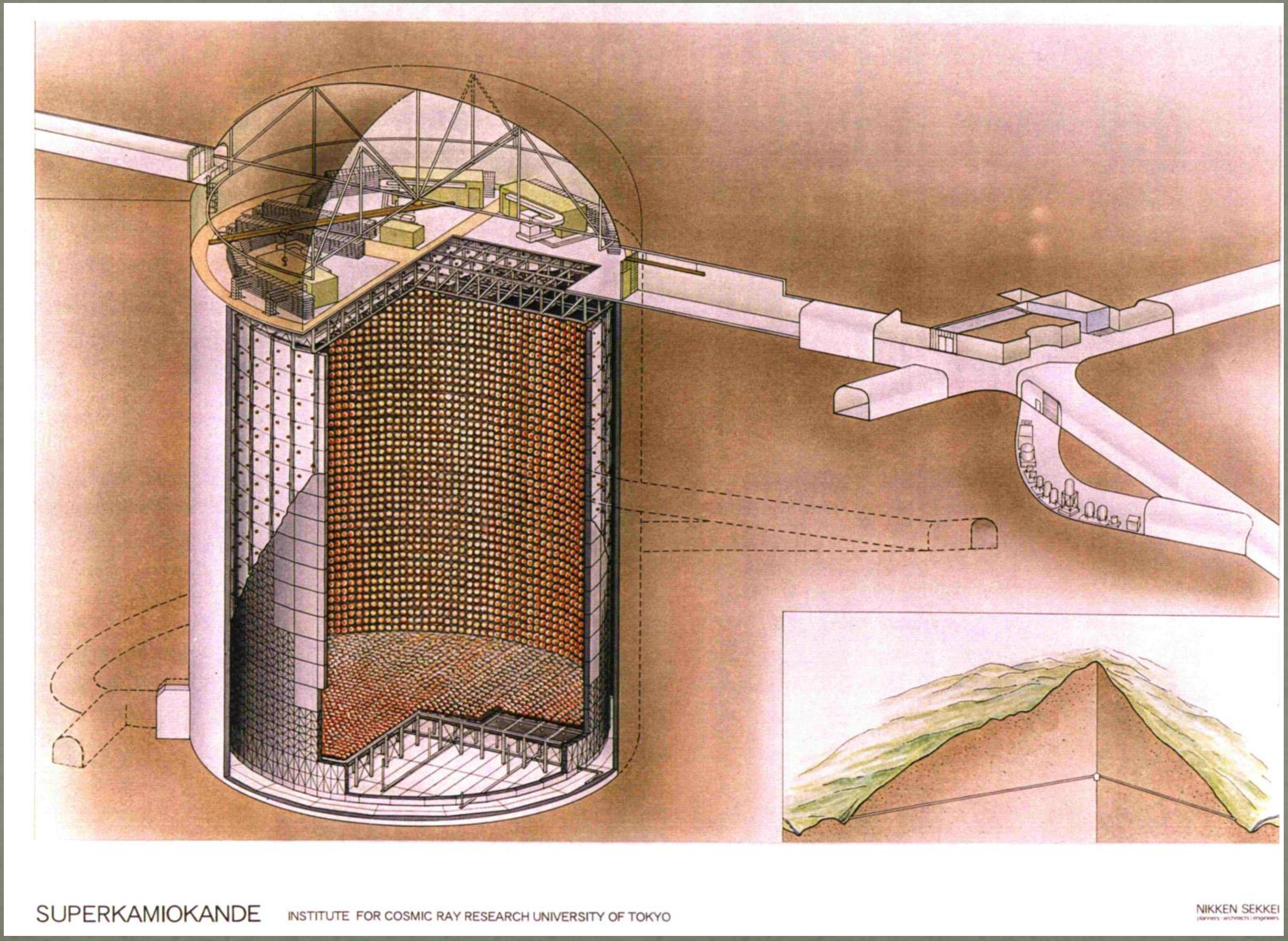

SK use electron scattering and see the Cerenkov light, and measure ν direction

Solar ν

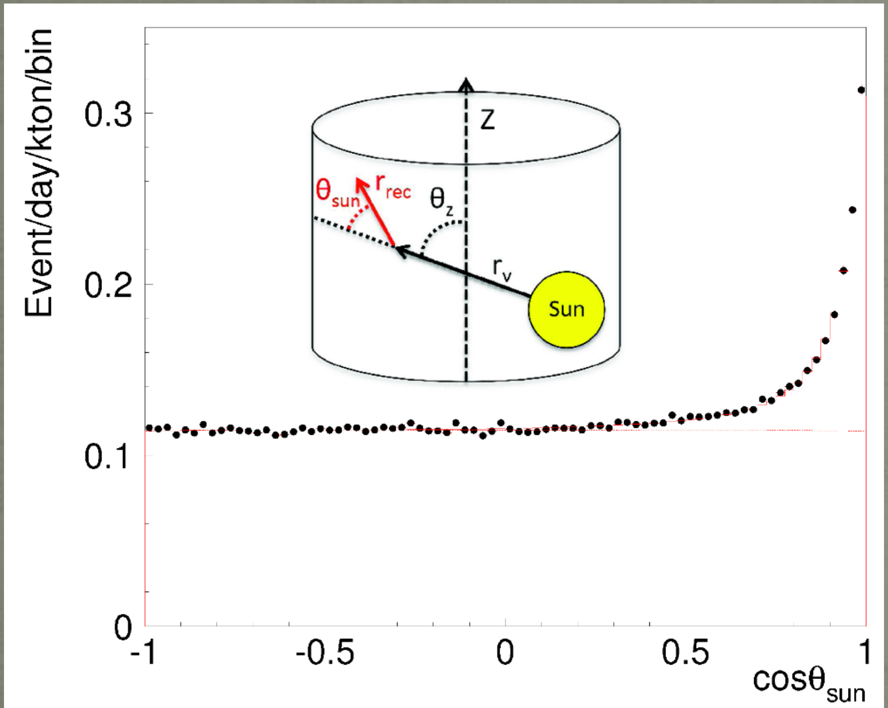

Atmospheric ν

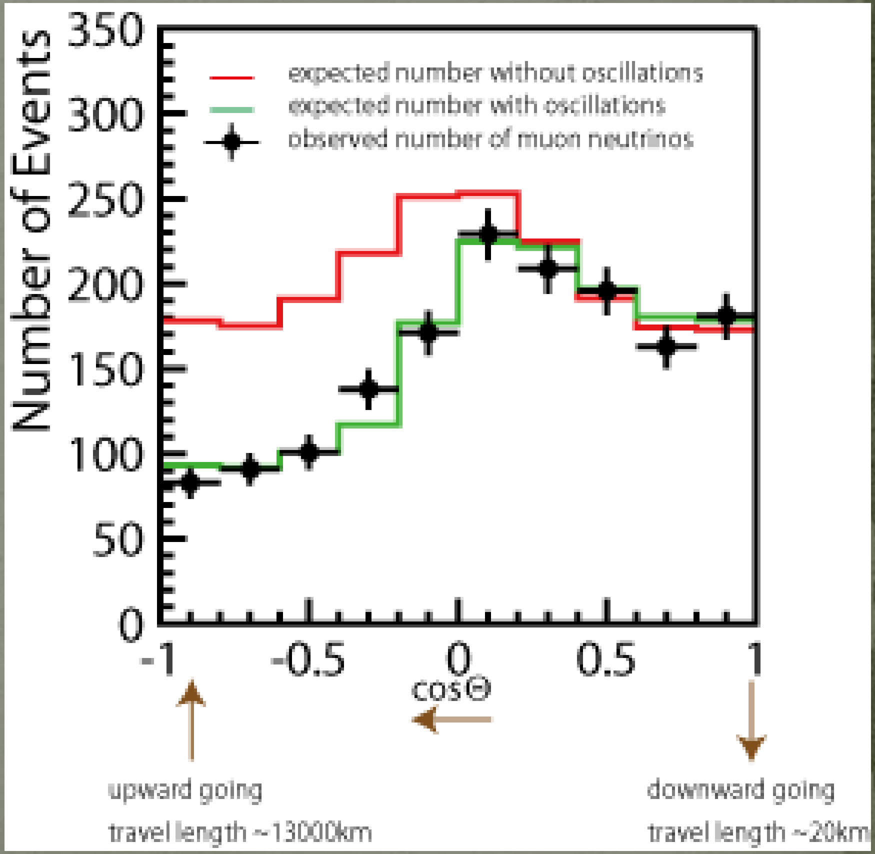

Neutrino oscillation using nuclear reactors

Daya Bay Experiment: Layout

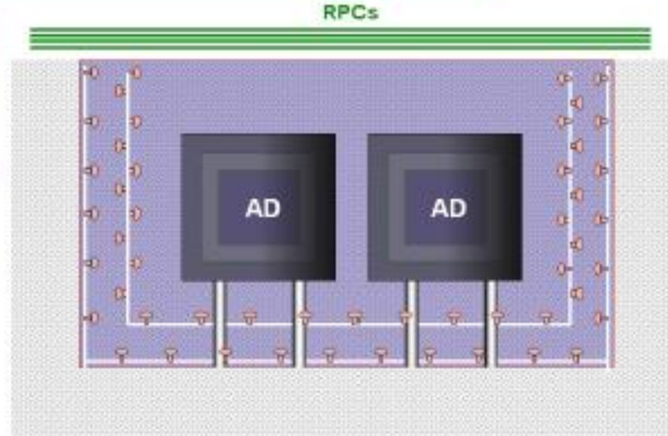

- Relative measurement to cancel Corr. Syst. Err.
  - 2 near sites, 1 far site
- Multiple AD modules at each site to reduce Uncorr. Syst. Err.
  - Far: 4 modules, near: 2 modules
- Multiple muon detectors to reduce veto eff. uncertainties
  - Water Cherenkov: 2 layers
  - RPC: 4 layers at the top + telescopes

Two ADs Installed in Hall 1

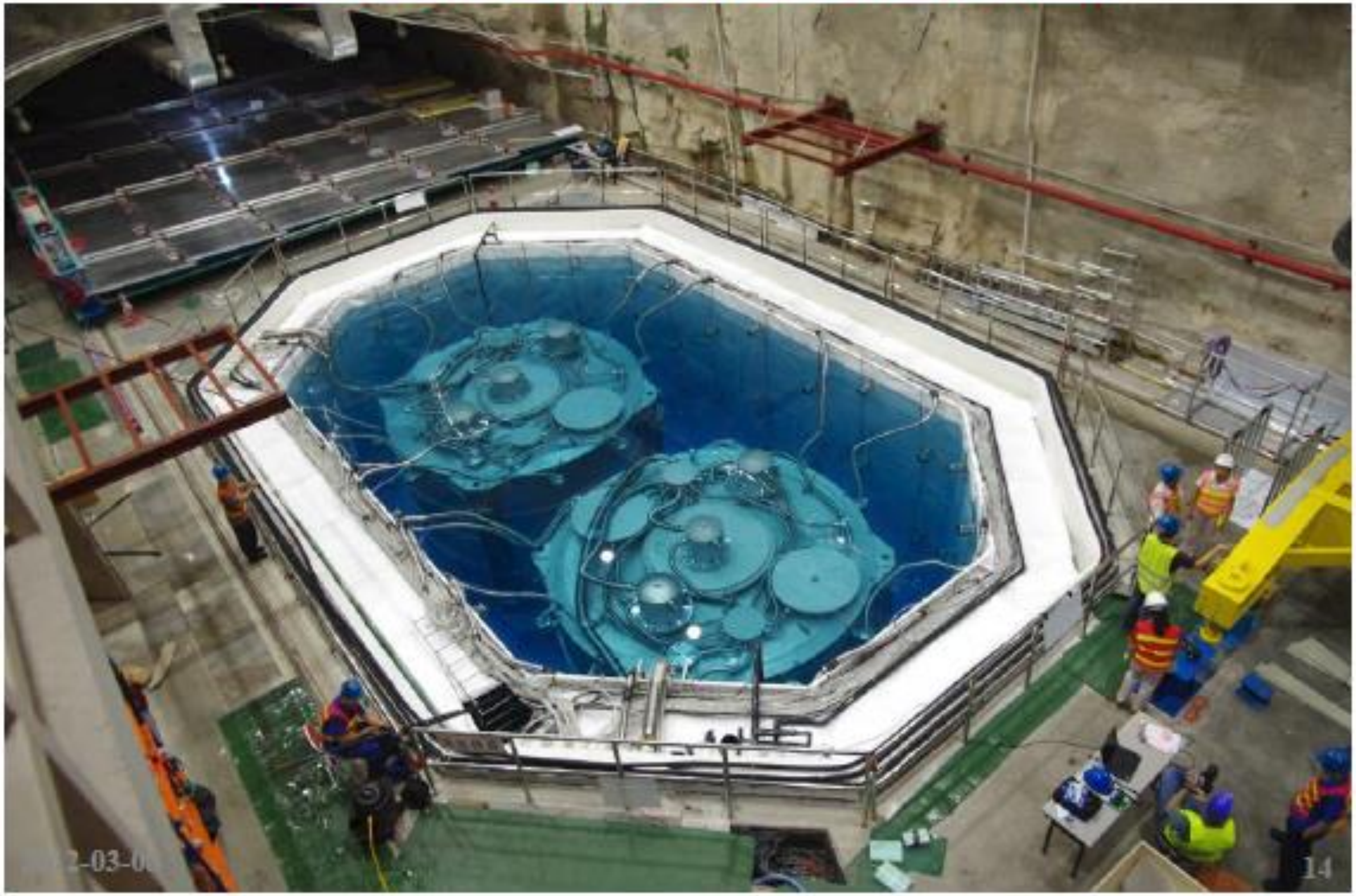

Final comments

Simulations for detector response as well as for physics results is quite important, although I haven't included them in the present lecture.

I would really recommend and ask you to train you easily carry these simulations.

An example of a simulation of physics results

In E137, invariant mass distribution of two tracks assumed to $\pi\pi$, for the event sample of the summed momentum directing to the production target.

- Simulation well reproduced shape of the tail, even for a small structure around 600 MeV.
- This got us confirm that we were doing a real KL measurement.
- This provided us pure π, μ, e samples by taking a specific mass region, and the sample s were quite useful for calibrations of PID detectors.
- The peak is on the KL mass, and was used for the normalization of other modes.

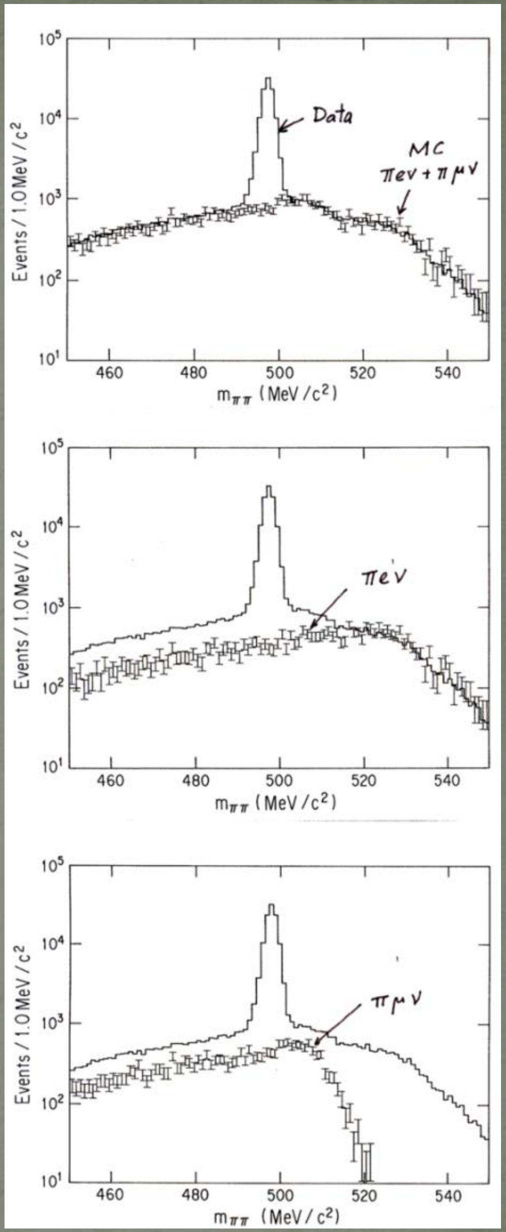

Simulation is also crucial for a detector design

Spectrum obtained from a 5.62 cm-squared NaI(Tl) crystal using 2.167 MeV photons from ^{38}K.
Not simple, but can be perfectly reproduced by Giant.

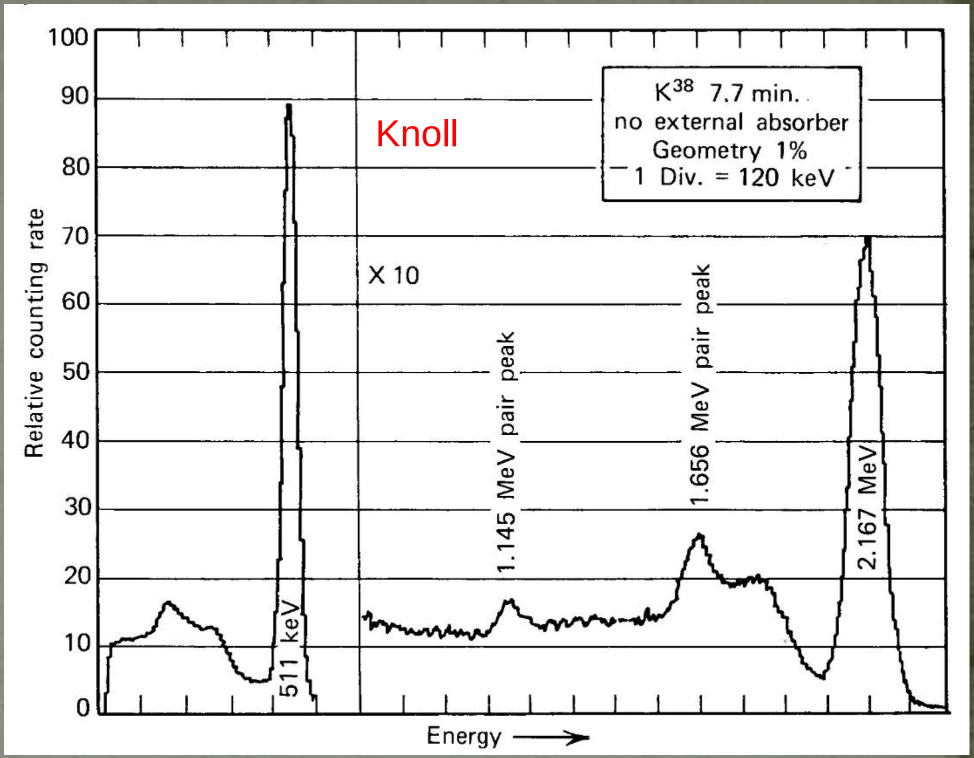

Training for a simulation code such as Giant must be fruitful for your future.